carotid atherosclerosis, and therefore yielded inconsistent findings [2,16–21].

We have previously established the plaque score (PS) as an indicator of the severity of carotid atherosclerosis, and have investigated the relationships between this score and classical risk factors for CVD [22] and C-reactive protein [23], silent brain infarction [9], platelet accumulation in the carotid arteries [24] and future ischaemic cerebrovascular disease [14]. In the present study, we used the PS and several other indicators to estimate the severity of carotid atherosclerosis, and we investigated the relationship between cICAM-1 or cP-selectin levels and the severity of carotid atherosclerosis.

MATERIALS AND METHODS

Subjects

A total of 301 outpatients over 40 years old, who were being treated for classical risk factors and/or secondary prevention of CVD at the Department of Internal Medicine of Osaka University Hospital, were investigated for carotid atherosclerosis and provided blood samples. Patients were excluded from the study if they had experienced a clinical cardiovascular event in the previous year or if another disease that could increase the cICAM-1 or cP-selectin level was present, i.e. malignancy, collagen disease, chronic renal failure, infection or hepatic disease [25]. None of the subjects were receiving anti-oxidant vitamin supplements, oestrogen therapy or steroid therapy. Patients gave written informed consent to provide blood samples and participate in the study. The study was approved by the local ethics committees.

Risk factors for CVD

Hypertension was defined as a systolic blood pressure $\geqslant$ 140 mmHg and/or a diastolic blood pressure $\geqslant$ 90 mmHg, or the current use of antihypertensive medications. Hypercholesterolaemia was defined as total cholesterol level $\geqslant$ 220 mg/dl or the current use of cholesterol-lowering agents. Diabetes mellitus was defined as a glycated haemoglobin (HbA_{1c}) level $\geqslant$ 5.8 % or the current use of oral hypoglycaemic agents. Patients were considered to be smokers if they were current smokers or had stopped smoking less than 1 month before enrolment in the study. Cigarette pack-years were calculated for each patient as a measure of cumulative smoking exposure. Patients were considered to have CVD if they had a prior history of ischaemic heart disease, cerebrovascular disease, aortic aneurysm or peripheral vascular disease. Patients were defined as taking antiplatelet therapy if they were being treated with aspirin or ticlopidine.

Evaluation of carotid atherosclerosis and measurement of cICAM-1 and cP-selectin levels

High-resolution B-mode ultrasonography was performed with a 7.5-MHz duplex-type scanner (Hitachi EUB-450, 555) to evaluate carotid atherosclerosis. The upper limit of normal for the intima-media thickness (IMT) was defined as 1.0 mm [22], and lesions with an IMT $\geqslant$ 1.1 mm were defined as atheromatous plaques. We used the following indicators to assess the severity of carotid atherosclerosis: (1) maximum IMT measured in mm at the thickest point (including plaque) of the near and far walls of both carotid arteries, (2) the number of plaques in both carotid arteries, (3) the PS (calculated by summing all plaque thicknesses measured in both carotid arteries, as shown in Figure 1) [22], and (4) the maximum stenosis (calculated by measuring the residual luminal diameter and the original diameter at the site of maximum stenosis and dividing the difference by the original diameter, with the result being reported as a percentage).

Blood samples were collected into tubes containing citric acid and EDTA, and were stored at −80 °C after centrifugation. The stored serum samples were assayed for cICAM-1, whereas the stored plasma samples were assayed for cP-selectin. Commercially available monoclonal antibody-based ELISA kits (R & D Systems, Minneapolis, MN, U.S.A.) were used for the determination of cICAM-1 and cP-selectin levels.

Statistical analysis

Data for the cICAM-1 and cP-selectin levels showed a normal distribution, whereas the maximum IMT, the number of plaques and the PS showed a skewed distribution. For univariate analysis, Spearman's rank-order correlation coefficients were determined to assess the association between cICAM-1 or cP-selectin level and the parameters of carotid atherosclerosis, i.e. maximum IMT, number of plaques and PS. The associations between

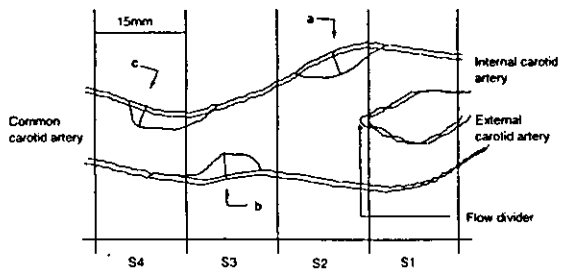

Figure 1 Diagram of carotid bifurcation and PS measurement obtained from B-mode ultrasonography

PS was calculated by summing all plaque thicknesses in mm in each segment on both sides (a + b + c + contralateral plaques). The carotid artery was divided into four parts, each 15 mm in length, from the flow divider (S1 to S4).

measured risk factors and PS were evaluated similarly. Differences of PS and the levels of circulating adhesion molecules in relation to categorical risk factors were evaluated by the Mann-Whitney *U* test and the unpaired *t* test respectively. Pearson's test was used to evaluate the relationship between cICAM-1 and cP-selectin levels, as well as those between the levels of these molecules and age. Patients were classified into four groups on the basis of the severity of carotid atherosclerosis: no disease (PS = 0), mild disease (PS = 1.1–5.0), moderate disease (PS = 5.1–10) and severe disease (PS > 10) [9,14,24]. One-way ANOVA was performed with Scheffé's multiple comparison test to assess differences in cICAM- and cP-selectin levels between these four groups. Patients were also classified into three groups on the basis of their maximum stenosis, i.e. no carotid atherosclerosis, less than 50 % stenosis and 50 % or more stenosis, after which the differences in cICAM-1 and cP-selectin levels between these three groups were similarly evaluated. To evaluate the differences, cICAM-1 and cP-selectin levels were adjusted for classical risk factors, statin use and a history of CVD. For multivariate analysis, multiple linear regression analysis was performed using each carotid atherosclerosis parameter as a dependent variable, while the age, sex, cigarette pack-years, presence/absence of hypertension, diabetes, hypercholesterolaemia, statin use, a history of CVD and the levels of circulating adhesion molecules were used as the predictive variables. The values of the maximum IMT, number of plaques and PS were log-transformed to normalize their distribution. 0.1 was assigned when number of plaques was 0, and 1.0 was assigned when PS was 0. All *P* values calculated were two-tailed and $P < 0.05$ was considered significant. All statistical analyses were conducted using SPSS/Windows software, version 9.0J (SPSS Japan Inc., Tokyo, Japan).

RESULTS

The clinical characteristics of the subjects are shown in Table 1. Of the 301 patients, 227 (75 %) had carotid atherosclerosis, and 105 (35 %) had a history of CVD and most of them were on antiplatelet therapy. In outpatients who were treated for hypertension, hypercholesterolaemia and diabetes mellitus, there were no significant differences in cICAM-1 and cP-selectin levels between the patients with or without these classical risk factors. As expected, the cICAM-1 level of current smokers was higher than that of non-current smokers (244.0 ± 86.1 ng/ml versus 189.0 ± 71.5 ng/ml, $P = 0.007$). The difference for cP-selectin was also significant (46.7 ± 26.5 ng/ml versus 38.5 ± 21.4 ng/ml, $P = 0.03$). The cICAM-1 level was higher in men than in women (212.8 ± 83.0 ng/ml versus 182.6 ± 66.3 ng/ml, $P = 0.008$), but no sex difference was found for cP-selectin. There were no statistical associations between the levels of the circulating adhesion molecules and age, nor were there any significant differences in cICAM-1 and cP-selectin levels between subjects with or without statin use, antiplatelet therapy or a history of CVD. The associations between the levels of cICAM-1 or cP-selectin and age were not significant when they were adjusted for gender. There was a significant correlation between cICAM-1 and cP-selectin levels ($r = 0.292$, $P < 0.001$).

Table 1 Clinical characteristics of the patients ($n = 301$)

Age, blood pressure, cholesterol, fasting blood glucose, HbA_{1c}, cigarette pack-years, plaque number, PS and circulating levels of adhesion molecules are expressed as the means ± S.D. Values shown in square brackets and parentheses are median values and number of patients respectively.

Characteristic	Value
Classical risk factors for CVD	
Age (years) (range)	64.0 ± 9.1 (40–88)
Male	53 %
Hypertension	68 %
Systolic/diastolic blood pressure (mmHg)	136 ± 17/80 ± 11
Hypercholesterolaemia	48 %
Total cholesterol/HDL cholesterol (mg/dl)	207 ± 32/55 ± 17
Statin use	26 %
Diabetes mellitus	18 %
Fasting blood glucose (mg/dl)	104 ± 26
HbA_{1c} (%)	5.3 ± 0.9
Current smoker	17 %
Cigarette pack-years	11.1 ± 22.2
History of CVD	35 %
Antiplatelet medication	33 %
Severity of carotid atherosclerosis	
Maximum IMT (mm)	1.9 ± 1.2 [1.5]
Number of plaques	2.7 ± 2.8 [2.0]
PS	4.8 ± 5.4 [2.9]
Maximum stenosis (0 %, < 50 %, ≥ 50 %)	(74, 200, 27)
cICAM-1 (ng/ml)	198.3 ± 76.8
cP-selectin (ng/ml)	39.9 ± 22.5

cICAM-1 and cP-selectin levels are shown in relation to the PS and maximum stenosis in Tables 2 and 3 respectively. Because the PS involves the factors of the number of plaques and maximum IMT, we showed Table 2 as a representative of the indicators. Unlike cICAM-1, cP-selectin did not increase until carotid atherosclerosis was severe (PS > 10). The cICAM-1 level of the severe group (PS > 10) was significantly higher than those of the group without atherosclerosis (PS = 0) and the group with mild atherosclerosis (PS = 1.1–5.0), whereas the cP-selectin level of the severe group was significantly higher than in all of the other three groups. The differences remained significant after adjustment for

Table 2 cICAM-1 and cP-selectin levels with respect to atherosclerosis categories

Values (except adjusted ones) are expressed as the means ± S.D. The adjusted values are expressed as the means ± S.E.M. *Adjusted for age, sex, smoking, hypertension, hypercholesterolaemia, statin use, diabetes mellitus and antiplatelet medication. †cICAM-1 levels in the severe disease group were significantly higher than levels in the none and mild disease groups ($P < 0.05$), but a significant difference was not found for the moderate disease group. ‡The differences remained significant after adjustment for classical risk factors, statin use and antiplatelet medication ($P < 0.05$). §cP-selectin levels in the severe disease group were higher than levels in the none, mild and moderate disease groups ($P < 0.05$).

Disease category	cICAM-1 (ng/ml)	Adjusted cICAM-1 (ng/ml)*	cP-selectin (ng/ml)	Adjusted cP-selectin (ng/ml)*
None ($n = 74$)	186.3 ± 80.7	188.2 ± 9.3	38.0 ± 24.5	38.0 ± 2.8
Mild ($n = 127$)	187.2 ± 75.1	188.1 ± 6.6	39.1 ± 19.7	39.2 ± 2.0
Moderate ($n = 49$)	218.3 ± 74.4	212.1 ± 11.0	35.9 ± 22.8	34.8 ± 3.3
Severe ($n = 51$)	224.2 ± 69.0†	227.8 ± 11.2‡	48.5 ± 24.5§	49.4 ± 3.4‡

Table 3 cICAM-1 and cP-selectin levels with respect to maximum stenosis

Values (except adjusted ones) are expressed as the means ± S.D. Adjusted values are expressed as the means ± S.E.M. *Adjusted for age, sex, smoking, hypertension, hypercholesterolaemia, statin use, diabetes mellitus and antiplatelet medication. cICAM-1 levels had a tendency to increase in parallel ($P = 0.067$), but the difference in the levels showed no statistical significance. †cP-selectin levels were higher in patients with 50% or more stenosis than in patients without carotid atherosclerosis and in patients with less than 50% stenosis ($P < 0.05$). ‡The difference remained significant after adjustment for classical risk factors, statin use and antiplatelet medication ($P < 0.05$).

Stenosis	cICAM-1 (ng/ml)	Adjusted cICAM-1 (ng/ml)*	cP-selectin (ng/ml)	Adjusted cP-selectin (ng/ml)*
0% ($n = 74$)	186.1 ± 80.2	190.3 ± 9.3	37.9 ± 24.3	38.1 ± 2.8
< 50% ($n = 200$)	199.2 ± 72.9	198.7 ± 5.4	38.9 ± 20.5	38.9 ± 1.6
⩾ 50% ($n = 27$)	225.9 ± 89.9	221.3 ± 14.8	53.2 ± 27.5†	52.2 ± 4.4‡

classical risk factors, statin use and antiplatelet medication (Table 2). When the number of plaques or maximum IMT was used as an indicator of carotid atherosclerosis, the results (not shown) were similar to those in Table 2. When maximum stenosis was used as an indicator of carotid atherosclerosis, cP-selectin levels were higher in patients with 50% or more stenosis than in patients without carotid atherosclerosis or patients with less than 50% stenosis. The difference remained significant after adjustment for classical risk factors, statin use and antiplatelet medication. cICAM-1 levels tended to increase in parallel with stenosis, although the trend was not statistically significant (Table 3).

Relationships between risk factors (including cICAM-1 and cP-selectin) and the PS are shown in Table 4. As expected, the PS of patients with classical risk factors and a history of CVD was higher than that in patients without these factors. The influence of cICAM-1 on the PS was similar to the influence of systolic blood pressure, high-density lipoprotein (HDL) cholesterol, fasting blood glucose, HbA_{1c} or cigarette pack-years. The influence of cP-selectin was weaker than that of the above risk factors, but it was still statistically significant. Diastolic blood pressure and total cholesterol were not significantly related to PS. When the predictive value of cICAM-1 or cP-selectin levels for the PS was compared with that of classical risk factors using multivariate regression analysis, the relationship between the cICAM-1 level and PS remained significant even after accounting for

Table 4 Relationships between PS and risk factors, including cICAM-1 and cP-selectin levels

The values shown are correlation coefficients between measured risk factors and PS, and mean ± S.D. for PS according to the presence or absence of categorical risk factors. n.s., not significant.

Risk factor for atherosclerosis	PS	*P* value
Age (years)	$r = 0.381$	< 0.001
Men/women	5.8 ± 6.0/3.6 ± 4.4	0.001
Hypertension (yes/no)	5.4 ± 3.8/3.2 ± 3.8	0.002
Systolic blood pressure	$r = 0.196$	0.001
Diastolic blood pressure	$r = -0.019$	n.s.
Hypercholesterolaemia (yes/no)	5.3 ± 5.5/4.3 ± 5.3	0.011
Total cholesterol	$r = 0.055$	n.s.
HDL cholesterol	$r = -0.167$	0.004
Statin use (yes/no)	5.6 ± 5.2/4.4 ± 5.4	0.01
Diabetes mellitus (yes/no)	7.1 ± 5.4/4.3 ± 5.3	< 0.001
Fasting blood glucose	$r = 0.197$	0.001
HbA_{1c}	$r = 0.239$	< 0.001
Current smoking (yes/no)	6.2 ± 6.0/4.5 ± 5.2	0.022
Cigarette pack-years	$r = 0.199$	0.001
History of CVD (yes/no)	6.1 ± 5.6/4.1 ± 5.2	0.001
cICAM-1	$r = 0.208$	< 0.001
cP-selectin	$r = 0.126$	0.03

Table 5 Results of multivariate regression analysis for PS

Variable	β (95% CI)	β (95% CI)
Age	0.33 (0.232–0.431)	0.34 (0.236–0.437)
Sex	0.12 (0.002–0.231)	0.11 (−0.005–0.23)
Hypertension	0.15 (0.047–0.25)	0.14 (0.039–0.239)
Diabetes	0.12 (0.017–0.223)	0.12 (0.017–0.225)
Hypercholesterolaemia	0.14 (0.008–0.264)	0.14 (0.006–0.263)
Statin use	0.10 (−0.027–0.23)	0.097 (−0.033–0.228)
Cigarette pack-years	0.060 (−0.05–0.171)	0.078 (−0.032–0.19)
History of CVD	0.075 (−0.029–0.18)	0.074 (−0.032–0.179)
cICAM-1	0.10 (0.001–0.205)	
cP-selectin		0.065 (−0.037–0.167)

the contribution of several classical risk factors (i.e. age, sex, hypertension, hypercholesterolaemia and diabetes mellitus), but the relationship for cP-selectin was no longer significant (Table 5).

With regard to the relationship between cICAM-1 or cP-selectin and other indicators, the cICAM-1 level was related to the maximum IMT ($r=0.22$, $P=0.001$) and to the number of plaques ($r=0.23$, $P=0.001$) by univariate analysis. When multivariate analysis was done, the relationship for the number of plaques [$\beta=0.110$, confidence interval (CI), 0.007–0.213] and maximum IMT ($\beta=0.114$; CI, 0.01–0.219) remained significant after accounting for the contribution of several classical risk factors. cP-selectin levels were related to maximum IMT ($r=0.15$, $P=0.008$), but not to the number of plaques, on univariate analysis. However, multivariate analysis did not confirm the relationship with maximum IMT.

DISCUSSION

A previous large-scale study showed that cICAM-1 levels were elevated in patients who had carotid atherosclerosis when compared with controls who had a normal IMT [2], while another study showed a significant relationship between cICAM-1 and the severity of carotid atherosclerosis (based on the mean IMT) [21]. However, studies that used the maximum IMT or maximum stenosis as an indicator have found no relationship with cICAM-1 [17–21]. The present study showed that cICAM-1 levels were related to the number of carotid plaques, maximum IMT and the PS. In contrast, there was no significant difference in cICAM-1 levels between groups that were stratified according to maximum stenosis. Because the present study was cross-sectional, we could not draw conclusions about the direction of association between cICAM-1 levels and carotid atherosclerosis. However, it is well known that adhesion molecules play important roles in the development of atherosclerosis and it has been reported that, unlike other adhesion molecules, ICAM-1 expression on endothelial cells is selectively upregulated by shear stress [26]. Strong focal expression of ICAM-1 is seen at the carotid bifurcation in patients with no or low-grade stenosis [27], whereas cICAM-1 levels are reported to increase in the early stage of carotid atherosclerosis [2]. Although the source of cICAM-1 in the serum is uncertain, circulating forms of adhesion molecules may be derived from vascular wall components, including endothelial and smooth muscle cells [28]. In the present study, atherosclerotic plaque was defined as an IMT $\geqslant$ 1.1 mm based on our previous study [22], which is in accordance with those in several other studies [13,29]. Small atherosclerotic plaques in early stages of atherosclerosis comprise smooth muscle cells and macrophage-derived foam cells [30], and the macrophage is transendothelial migrated forms of a leucocyte [31]. The present study showed that cICAM-1 levels are significantly associated not only with maximum IMT but also with the number of plaques and PS. Taken together, these findings indicate that cICAM-1 levels may partly reflect the total extent of arterial involvement by atherosclerosis rather than the rate of carotid stenosis, and that elevation of cICAM-1 levels may precede the development of stenosis, which may help to explain previous inconsistent findings in studies based on different measures of carotid disease.

The strength of the relationship between cICAM-1 and cP-selectin levels in all of our subjects ($r=0.292$, $P<0.001$) was similar to that shown by a population-based study ($r=0.23$, $P=0.001$) [6], and that in patients with stable coronary syndrome ($r=0.314$, $P=0.007$) [32]. It was also similar to that found between cICAM-1 and circulating E-selectin ($r=0.22$, $P=0.0001$) and between cICAM-1 and circulating vascular cell-adhesion molecule-1 ($r=0.17$, $P=0.0001$) in a population-based study [2]. Focal expression of E-selectin in carotid arteries with no or low-grade stenosis is reported to be far weaker than expression of ICAM-1 [27]. Because we found that cP-selectin levels did not increase significantly until the advanced stage of carotid atherosclerosis, P-selectin may also show weak expression in carotid arteries with no or low-grade stenosis, and the increase of cP-selectin during the atherosclerotic process may follow the elevation of cICAM-1. Consistent with these findings, cP-selectin levels were previously reported to be higher in patients with carotid stenosis than in control subjects [20].

P-selectin is an adhesion molecule that supports the adherence of rolling leucocytes to the endothelium, and such adhesion is reinforced by ICAM-1-mediated bonding [31]. P-selectin and ICAM-1 are reported to be key adhesion molecules in the promotion of atherosclerosis [33–36], and expression of P-selectin in the endothelium overlying atherosclerotic plaques in humans is strongly correlated with ICAM-1 expression [37]. However, P-selectin is also expressed on the surface of activated platelets [38], and a previous study has

suggested that an elevated cP-selectin level may be a marker of platelet activation [39]. In fact, the origin of these circulating adhesion molecules has not yet been fully clarified. The increase of cP-selectin in patients with severe carotid atherosclerosis may be partly derived from activated platelets [39], since an experimental study has shown that P-selectin expression may play a role in platelet aggregation stimulated by pulsatile shear stress, which resembles blood flow in stenotic arteries [40]. This is also in accordance with our previous finding of increased platelet accumulation in the carotid arteries of patients with 50 % or more stenosis and a PS > 10 [24]. Because carotid plaque growth is accelerated by plaque fissuring and thrombosis when a plaque causes more than 40 % diameter reduction [41], the increase of cP-selectin may be a consequence of silent plaque rupture and platelet activation.

Because the present study focused on outpatients with classical risk factors for CVD, the confounding effects of antiplatelet and statin medication should be considered. Statins were used more frequently in patients with more severe carotid atherosclerosis in the present study. Because statins are reported to reduce cP-selectin levels [42], statin use may lead to an underestimation of true levels of cP-selectin in advanced carotid atherosclerosis and bias our findings toward a null result. The population of patients on antiplatelet medication was equal to that of those with a history of CVD. The relationship between cICAM-1 and the severity of carotid atherosclerosis remained significant, even after adjusting for the contribution of classical risk factors including statin use and history of CVD.

In conclusion, we found that cICAM-1 levels increased in parallel with the total extent of carotid arterial affected by atherosclerosis, but that cP-selectin levels did not increase until the stage of advanced carotid atherosclerosis, and both proteins predicted the severity of carotid atherosclerosis independently of classical risk factors. Ultrasonographic examination, which uses several scales to estimate the severity of carotid atherosclerosis, including measurement of carotid plaques, may be used to assess the origin of circulating forms of the other adhesion molecules.

REFERENCES

1 Ross, R. (1999) Atherosclerosis: an inflammatory disease. N. Engl. J. Med. 340, 115–126
2 Hwang, S.-J., Ballantyne, C. M., Sharrett, A. R. et al. (1997) Circulating adhesion molecules VCAM-1, ICAM-1, and E-selectin in carotid atherosclerosis and incident coronary heart disease cases: the Atherosclerosis Risk In Communities (ARIC) study. Circulation 96, 4219–4225
3 Ridker, P. M., Hennekens, C. H., Roitman-Johnson, B., Stampfer, M. J. and Allen, J. (1998) Plasma concentration of soluble intercellular adhesion molecule 1 and risks of future myocardial infarction in apparently healthy men. Lancet 351, 88–92
4 Blann, A. D., Faragher, E. B. and McCollum, C. N. (1997) Increased soluble P-selectin following myocardial infarction: a new marker for the progression of atherosclerosis. Blood Coagulation Fibrinolysis 8, 383–390
5 Blann, A. D. and McCollum, C. N. (1998) Increased soluble P-selectin in peripheral artery disease: a new marker for the progression of atherosclerosis. Thromb. Haemostasis 80, 1031–1032
6 Ridker, P. M., Buring, J. E. and Rifai, N. (2001) Soluble P-selectin and the risk of future cardiovascular events. Circulation 103, 491–495
7 Ridker, P. M. (2001) Role of inflammatory biomarkers in prediction of coronary heart disease. Lancet 358, 946–948
8 Bots, M. L., Hofman, A. and Grobbee, D. E. (1994) Common carotid intima-media thickness and lower extremity arterial atherosclerosis. The Rotterdam Study. Arterioscler. Thromb. 14, 1885–1891
9 Hougaku, H., Matsumoto, M., Handa, N. et al. (1994) Asymptomatic carotid lesions and silent cerebral infarction. Stroke 25, 566–570
10 Nagai, Y., Metter, E. J., Earley, C. J. et al. (1998) Increased carotid artery intimal-medial thickness in asymptomatic older subjects with exercise-induced myocardial ischemia. Circulation 98, 1504–1509
11 Tanaka, H., Nishino, M., Ishida, M., Fukunaga, R. and Sueyoshi, K. (1992) Progression of carotid atherosclerosis in Japanese patients with coronary artery disease. Stroke 23, 946–951
12 Bots, M. L., Hoes, A. W., Koudstaal, P. J., Hofman, A. and Grobbee, D. E. (1997) Common carotid intima-media thickness and risk of stroke and myocardial infarction: the Rotterdam Study. Circulation 96, 1432–1437
13 Chambless, L. E., Heiss, G., Folsom, A. R. et al. (1997) Association of coronary heart disease incidence with carotid arterial wall thickness and major risk factors: the Atherosclerosis Risk in Communities (ARIC) Study, 1987–1993. Am. J. Epidemiol. 146, 483–494
14 Handa, N., Matsumoto, M., Maeda, H., Hougaku, H. and Kamada, T. (1995) Ischemic stroke events and carotid atherosclerosis. Results of the Osaka Follow-up Study for Ultrasonographic Assessment of Carotid Atherosclerosis (the OSACA Study). Stroke 26, 1781–1786
15 O'Leary, D. H., Polak, J. F., Kronmal, R. A., Manolio, T. A., Burke, G. L. and Wolfson, Jr, S. K. (1999) Carotid-artery intima and media thickness as a risk factor for myocardial infarction and stroke in older adults. Cardiovascular Health Study Collaborative Research Group. N. Engl. J. Med. 340, 14–22
16 Blann, A. D., Seigneur, M., Boisseau, M. R., Taberner, D. A. and McCollum, C. N. (1996) Soluble P selectin in peripheral vascular disease: relationship to the location and extent of atherosclerotic disease and its risk factors. Blood Coagulation Fibrinolysis 7, 789–793
17 Blann, A. D., Farrell, A., Picton, A. and McCollum, C. N. (2000) Relationship between endothelial cell markers and arterial stenosis in peripheral and carotid artery disease. Thromb. Res. 97, 209–216
18 DeGraba, T. J., Sirén, A.-L., Penix, L. et al. (1998) Increased endothelial expression of intercellular adhesion molecule-1 in symptomatic versus asymptomatic human carotid atherosclerotic plaque. Stroke 29, 1405–1410
19 Fassbender, K., Bertsch, T., Mielke, O., Muhlhauser, F. and Hennerici, M. (1999) Adhesion molecules in cerebrovascular diseases. Evidence for an inflammatory endothelial activation in cerebral large- and small-vessel disease. Stroke 30, 1647–1650
20 Frijns, C. J., Kappelle, L. J., van Gijn, J., Nieuwenhuis, H. K., Sixma, J. J. and Fijnheer, R. (1997) Soluble adhesion molecules reflect endothelial cell activation in ischemic stroke and in carotid atherosclerosis. Stroke 28, 2214–2218
21 Rohde, L. E., Lee, R. T., Rivero, J. et al. (1998) Circulating cell adhesion molecules are correlated with ultrasound-based assessment of carotid atherosclerosis. Arterioscler. Thromb. Vasc. Biol. 18, 1765–1770

22 Handa, N., Matsumoto, M., Maeda, H. et al. (1990) Ultrasonic evaluation of early carotid atherosclerosis. Stroke 21, 1567–1572
23 Hashimoto, H., Kitagawa, K., Hougaku, H. et al. (2001) C-reactive protein is an independent predictor of the rate of increase in early carotid atherosclerosis. Circulation 104, 63–67
24 Moriwaki, H., Matsumoto, M., Handa, N. et al. (1995) Functional and anatomic evaluation of carotid atherothrombosis. A combined study of indium 111 platelet scintigraphy and B-mode ultrasonography. Arterioscler. Thromb. Vasc. Biol. 15, 2234–2240
25 Bevilacqua, M. P., Nelson, R. M., Mannori, G. and Cecconi, O. (1994) Endothelial-leukocyte adhesion molecules in human disease. Annu. Rev. Med. 45, 361–378
26 Nagel, T., Resnick, N., Atkinson, W. J., Dewey, C. F. and Gimbrone, M. A. (1994) Shear stress selectively upregulates intercellular adhesion molecule-1 expression in cultured human vascular endothelial cells. J. Clin. Invest. 94, 885–891
27 Endres, M., Laufs, U., Merz, H. and Kaps, M. (1997) Focal expression of intercellular adhesion molecule-1 in the human carotid bifurcation. Stroke 28, 77–82
28 Leeuwenberg, J. F., Smeets, E. F., Neefjes, J. J. et al. (1992) E-selectin and intercellular adhesion molecule-1 are released by activated human endothelial cells *in vitro*. Immunology 77, 543–549
29 Bots, M. L., Hofman, A. and Grobbee, D. E. (1997) Increased common carotid intima-media thickness. Adaptive response or a reflection of atherosclerosis? Findings from the Rotterdam Study. Stroke 28, 2442–2447
30 Fuster, V. (1997) Present concepts of coronary atherosclerosis-thrombosis, therapeutic implications and perspectives. Arch. Mal Coeur Vaiss 90, 41–47
31 Springer, T. A. (1994) Traffic signals for lymphocyte recirculation and leukocyte emigration: the multistep paradigm. Cell (Cambridge, Mass.) 76, 301–314
32 Parker, III, C., Vita, J. A. and Freedman, J. E. (2001) Soluble adhesion molecules and unstable coronary artery disease. Atherosclerosis 156, 417–424
33 Collins, R. G., Velji, R., Guevara, N. V., Hicks, M. J., Chan, L. and Beaudet, A. L. (2000) P-Selectin or intercellular adhesion molecule (ICAM)-1 deficiency substantially protects against atherosclerosis in apolipoprotein E-deficient mice. J. Exp. Med. 191, 189–194
34 Dong, Z. M., Brown, A. A. and Wagner, D. D. (2000) Prominent role of P-selectin in the development of advanced atherosclerosis in ApoE-deficient mice. Circulation 101, 2290–2295
35 Johnson, R. C., Chapman, S. M., Dong, Z. M. et al. (1997) Absence of P-selectin delays fatty streak formation in mice. J. Clin. Invest. 99, 1037–1043
36 Nageh, M. F., Sandberg, E. T., Marotti, K. R. et al. (1997) Deficiency of inflammatory cell adhesion molecules protects against atherosclerosis in mice. Arterioscler. Thromb. Vasc. Biol. 17, 1517–1520
37 Johnson-Tidey, R. R., McGregor, J. L., Taylor, P. R. and Poston, R. N. (1994) Increase in the adhesion molecule P-selectin in endothelium overlying atherosclerotic plaques. Co-expression with intercellular adhesion molecule-1. Am. J. Pathol. 144, 952–961
38 Wu, K. K. (1996) Platelet activation mechanisms and markers in arterial thrombosis. J. Intern. Med. 239, 17–34
39 Blann, A. D. and Lip, G. Y. (1997) Hypothesis: is soluble P-selectin a new marker of platelet activation? Atherosclerosis 128, 135–138
40 Merten, M., Chow, T., Hellums, J. D. and Thiagarajan, P. (2000) A new role for P-selectin in shear-induced platelet aggregation. Circulation 102, 2045–2050
41 Kiechl, S. and Willeit, J. (1999) The natural course of atherosclerosis. Part I: incidence and progression. Arterioscler. Thromb. Vasc. Biol. 19, 1484–1490
42 Murphy, R. T., Foley, J. B., Mulvihill, N., Crean, P. and Walsh, M. J. (2001) Impact of pre-existing statin use on adhesion molecule expression in patients presenting with acute coronary syndromes. Am. J. Cardiol. 87, 446–448

Received 15 October 2002/16 December 2002; accepted 6 February 2003
Published as Immediate Publication 6 February 2003, DOI 10.1042/CS20020290

Circ J 2003; **67:** 597–600

Carotid Atherosclerosis as a Risk Factor for Complex Aortic Lesions in Patients With Ischemic Cerebrovascular Disease

Yoshiomi Shimizu, MD; Kazuo Kitagawa, MD; Yoji Nagai, MD; Masako Narita, MD; Hidetaka Hougaku, MD; Tohru Masuyama, MD; Masayasu Matsumoto, MD*; Masatsugu Hori, MD

Aortic arch atherosclerotic lesions can cause ischemic cerebrovascular disease (ICVD). The association between carotid and aortic atherosclerosis was examined, and it was investigated whether noninvasive carotid evaluation aids in the identification of aortic lesions as potential ICVD risk. The subjects comprised 147 patients with ICVD who had undergone carotid ultrasonography and transesophageal echocardiography. Carotid and aortic arch atherosclerosis was evaluated by measuring the maximum intima–media thickness (IMT), with aortic IMT of at least 4 mm, mobile plaques and/or ulcers defined as complex aortic lesions with potential ICVD risk. Carotid IMT was linearly associated with aortic IMT ($r=0.53$, $p<0.001$), and the association was independent of traditional cardiovascular risk factors ($\beta=0.36$, $p<0.001$). Also, each 1 SD greater carotid IMT was associated with 4.2-fold (95% confidence interval: 2.5–7.0) higher likelihood of complex aortic lesions, with the likelihood little modified when controlling for cardiovascular risk factors. In particular, complex aortic lesions were found in 78% of patients with the highest carotid IMT tertile, compared with 14% of those with the lowest tertile ($p<0.05$). Based on these findings, carotid atherosclerosis is associated with aortic atherosclerosis, representing a risk factor for aortic lesions that are a potential ICVD risk. (*Circ J* 2003; **67:** 597–600)

Key Words: Aorta; Atherosclerosis; Carotid arteries; Ultrasound

The recent clinical advent of transesophageal echocardiography (TEE) has allowed identification of occult embolic sources in the cerebral arteries, greatly contributing to the diagnosis of ischemic cerebrovascular disease (ICVD). Although TEE is primarily performed for the identification of the source of cardiac embolism, aortic lesions found thereby have been associated with the risk for ICVD[1–3] In particular, advanced arch lesions, such as mobile plaques, ulcers and an intima–media thickness (IMT) greater than 4 mm, have been associated with the risk for cerebral embolism[4,5] On the basis of those studies, identification of aortic lesions may assist in clarifying the etiology of ICVD and, potentially, may prevent future events.

Carotid ultrasonography is a commonly used clinical tool for the diagnosis and risk assessment of ICVD because it enables noninvasive observation of atherosclerosis and an association between carotid and aortic atherosclerosis has been shown[6] In addition, TEE has shown that carotid artery stenosis often coexists in patients with aortic atheroma[7,8] However, advanced aortic lesions are frequently found in cases of ICVD without carotid stenosis. Accordingly, the factors predisposing to carotid and aortic atherosclerosis are not clearly separated, and whether carotid atherosclerosis is a marker for aortic lesions has not been determined. If noninvasive carotid imaging can identify complex aortic lesions, it may also provide additional information for the selection of candidates for TEE.

Carotid and aortic arch atherosclerosis is commonly evaluated by measuring the IMT on ultrasonography. The present study examined the association between carotid and aortic IMT in patients with ICVD, and investigated whether noninvasive carotid evaluation aids in the identification of complex aortic lesions that are a potential ICVD risk.

Methods

Subjects

The subjects for this investigation were enrolled from the ICVD patients admitted to Department of Internal Medicine and Therapeutics, Osaka University Hospital between July 1998 and August 2001. All patients had been referred from other clinics or departments for determination of the etiology of the ICVD and for its secondary prevention. During the study period, all ICVD patients underwent carotid ultrasonography and the majority of those also underwent TEE, except for those with the following criteria: (1) unequivocal etiology such as vertebral artery dissection and moyamoya disease, or (2) unlikely to benefit from TEE (eg, esophageal varices, terminal stages of malignancy). Additionally, because we wished to focus on the origin of the atherosclerosis, patients who had undergone carotid endarterectomy were excluded, as were those with Takayasu's and other arteritis conditions. Accordingly, patients with posterior circulation infarct and those with a recognized

(Received December 27, 2002; revised manuscript received March 25, 2003; accepted April 11, 2003)

*Department of Internal Medicine and Therapeutics, Osaka University Graduate School of Medicine, Osaka and *Department of Clinical Neuroscience and Therapeutics, Hiroshima University Graduate School of Biomedical Sciences, Hiroshima, Japan*

Mailing address: Kazuo Kitagawa, MD, PhD, Department of Internal Medicine and Therapeutics, Osaka University Graduate School of Medicine, 2-2 Yamadaoka, Suita, Osaka 565-0871, Japan. E-mail: kitagawa@medone.med.osaka-u.ac.jp

Table 1 Patients Characteristics

n	*147*
Age (years)	*64±10*
Sex (% men)	*69*
Hypertension (%)	*67*
Hyperlipidemia (%)	*48*
Diabetes mellitus (%)	*20*
Smoking habit (%)	*46*
Aortic IMT (mm)	*3.7±1.9*
Carotid IMT (mm)	*1.7±0.8*

IMT, intima–media thickness.

source of cardiac emboli were included in this study. After exclusion of 12 patients, based on our criteria, the study sample comprised 147 ICVD patients (age: 64±10 years), including 124 cases of ischemic stroke, 8 of transient ischemic attack and 15 of silent cerebral infarction.

This study conformed with the principles outlined in the Declaration of Helsinki, and informed consent was obtained from all subjects after the nature of procedures had been fully explained.

Carotid Ultrasonography

Duplex carotid ultrasonography was performed with a linear array 7.5 MHz transducer (SSA-260A, Toshiba Inc, Tokyo, Japan). In accordance with other studies, the degree of carotid atherosclerosis was evaluated by measuring the maximum IMT of the common carotid artery or its bifurcation.

Briefly, the subject lay supine in a darkened room, and the examinations were done with the head held in the midline position or slightly tilted to the side. For the evaluation of IMT, the transducer was manipulated so that the near and far arterial walls were parallel to the transducer footprint and the lumen diameter was maximized in the longitudinal plane. The section with greatest IMT was visually identified on the far wall, where the maximum IMT was evaluated as the distance between the lumen–intima interface and the media–adventitia interface. IMT was measured on the frozen frame of a suitable longitudinal image with the image magnified to achieve a higher resolution of detail. The contralateral carotid artery was examined following the same procedure, and the mean of both sides was used for analyses. Of note, the IMT measured in this study represents an indicator of earlier carotid atherosclerosis, and the increase per se does not pose a direct threat to the cerebral circulation.

Carotid evaluations were performed prior to TEE by stroke neurologists/cardiologists (Y.S., Y.N., M.N.) who were skilled in the procedure.

Transesophageal Echocardiography

TEE was performed in accordance with standard protocols. After topical anesthesia of the oropharynx, a multiplane probe (SONOS 5500, Hewlett Packard Inc, Andover, OH, USA) was inserted into the esophagus, and the aortic wall was observed cross-sectionally and longitudinally. Subsequently, the aortic IMT (Ao-IMT) was measured at its maximum site in the proximal arch, as the distance between the lumen–intima interface and the media–adventitia interface. It was measured on the frozen frame, perpendicular to the vascular walls. The measurements were performed on both cross-sectional and longitudinal frames, and the mean value was used for analyses. In referring to the literature[4,5] an Ao-IMT ≥4 mm, mobile plaques and/or ulcers were defined as complex lesions with a potential ICVD risk. Mobile plaques were characterized by intraluminally protruding lesions with mobile components, and ulcers were diagnosed by the presence of large, obvious excavations (≥2 mm in depth and ≥2 mm in length) on the surface, with a well-defined back wall at its base.

All evaluations were performed by skilled stroke neurologists/cardiologists. Because TEE was performed as part of the routine clinical workup, the examiners were not completely unaware of the carotid findings. Thus, to reinforce the objectivity of the diagnoses, the aortic findings were always interpreted by 3 attendant examiners, with the final diagnoses made by consensus.

Table 2 Risk Factors for the Thickening of Aortic and Carotid Intima–Media Thickness (IMT)

	Aortic IMT	*Carotid IMT*
Univariate		
Age	*0.46**	*0.29**
Sex (men/women)	*4.1±1.9/3.0±1.6**	*1.8±0.8/1.4±0.8**
Hypertension (yes/no)	*3.9±1.8/3.4±2.0*	*1.8±0.8/1.4±0.7**
Hyperlipidemia (yes/no)	*4.0±2.0/3.5±1.7*	*1.8±0.9/1.5±0.7**
Diabetes mellitus (yes/no)	*3.9±1.6/3.7±2.0*	*1.8±0.7/1.7±0.8*
Smoking habit (yes/no)	*4.3±1.8/3.3±1.9**	*1.9±0.9/1.5±0.7**
Multivariate		
Age	*0.47**	*0.27**
Sex (men = 1)	*0.11*	*0.07*
Hypertension	*0.04*	*0.23**
Hyperlipidemia	*0.16**	*0.19**
Diabetes mellitus	*0.02*	*0.07*
Smoking habit	*0.26**	*0.23**
(Model r^2)	*(0.34)*	*(0.25)*

*In univariate analyses, values represent correlation coefficients for continuous variables, and mean±SD for dichotomic variables. In multivariate analyses, values represent standardized regression coefficients. *p<0.05.*

Data Analyses

Risk factors for the thickening of both the aortic and carotid IMT were explored by correlation analysis and unpaired t-test, followed by multiple linear regression analysis. The risk factors considered were age, sex, hypertension (casual blood pressure ≥160/95 mmHg or on medication), diabetes mellitus (fasting plasma glucose ≥7.77 mmol/L or on medication), hyperlipidemia (serum total cholesterol ≥5.70 mmol/L or on medication), and smoking. Smoking status was evaluated from self-reports, with a smoker defined by current or past smoking of more than 10 cigarettes/day for more than 1 year. Linear regression analysis was also used to examine the association between aortic and carotid IMT. Subsequently, the ability of carotid IMT to identify complex aortic lesions was examined by logistic regression analyses. Chi-square test was used to compare the frequency of complex aortic lesions across the tertiles of carotid IMT. Data are presented as mean±SD unless otherwise specified, and a two-tailed p value <0.05 considered statistically significant. All analyses were performed using SPSS 9.0 (SPSS Japan Inc, Tokyo, Japan).

Results

Baseline Characteristics

Because all patients had preceding ICVD, the prevalence of traditional cardiovascular risk factors was generally high in the study sample, with approximately 50% of patients having hypertension, hyperlipidemia or smoking habit (Table 1). As measures for aortic and carotid atherosclerosis, the average aortic and carotid IMT was 3.7±1.9 mm and

Table 3 Multiple Regression Analyses of Aortic Intima–Media Thickness (IMT)

	Univariate	*Age and sex adjusted*	*All risk factors adjusted*
Carotid IMT	*0.53**	*0.40**	*0.36**
Age (years)		*0.33**	*0.37**
Sex (men=1)		*0.14**	*0.08*
Hypertension			*–0.04*
Hyperlipidemia			*0.09*
Diabetes mellitus			*–0.01*
Smoking habit			*0.18**
(Model r^2)	*(0.28)*	*(0.40)*	*(0.44)*

*Values represent standardized regression coefficients, *p<0.05.*

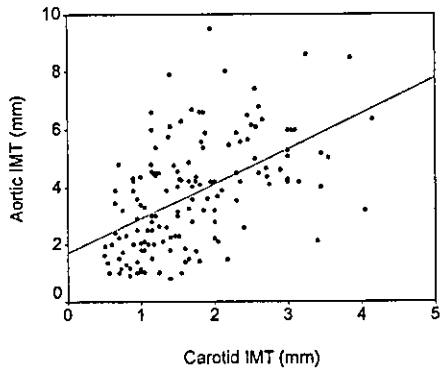

Fig 1. Association between aortic and carotid intima–media thickness (IMT). r=0.53, p<0.001. Aortic IMT = 1.69 + 1.22 × Carotid IMT

1.7±0.8 mm respectively.

Risk Factors for the Thickening of Aortic and Carotid IMT

Both aortic and carotid IMT were moderately correlated with age, and greater in men than in women (Table 2). Also, they were generally greater in patients with cardiovascular risk factors than in those without. By multiple regression analysis, age, hyperlipidemia and smoking habit were found to be independently associated with both aortic and carotid IMT. Additionally, hypertension had an independent association with carotid IMT, but not with aortic IMT.

Associations Between Aortic and Carotid IMT

A moderate linear association was found between aortic and carotid IMT (Table 3, Fig 1). Although quadratic and cubic terms were also examined, the explicable variance was similar to that obtained by the linear term. After adjusting for age and sex, carotid IMT remained significantly associated with aortic IMT. When all cardiovascular risk factors were considered for the model, carotid IMT, age and smoking habit were found to be independently associated with aortic IMT.

Identification of Complex Aortic Lesions by Carotid IMT

Given the association between aortic and carotid IMT, noninvasive carotid evaluation may be able to identify aortic lesions that are a potential ICVD risk. To examine this, we performed logistic regression analyses, with the existence of complex aortic lesions as an endpoint. Because the relative risk appeared to increase log-linearly with carotid IMT (data not shown), we computed the odds ratio associated with 1 SD increase in carotid IMT. By univariate analysis, each SD greater carotid IMT was associated with 4.2-fold higher likelihood for complex aortic lesions (Table 4). Furthermore, the likelihood was only slightly attenuated when adjusting for age and sex, and additional cardiovascular risk factors. In the model including all such risk factors, carotid IMT and age were found to be significant predictors for complex aortic lesions.

Table 4 Logistic Regression Analyses for Predicting Complex Aortic Lesions

	Univariate	*Age and sex adjusted*	*All risk factors adjusted*
Carotid IMT (/SD)	*4.2 (2.5–7.0)**	*3.6 (2.1–6.1)**	*3.2 (1.8–5.6)**
Age (/10 years)		*2.3 (1.4–3.7)**	*2.5 (1.5–4.1)**
Sex (men=1)		*1.5 (0.6–3.7)*	*1.1 (0.4–3.0)*
Hypertension			*1.1 (0.4–2.8)*
Hyperlipidemia			*1.2 (0.5-2.8)*
Diabetes mellitus			*1.3 (0.5-3.6)*
Smoking habit			*2.0 (0.8-5.2)*
(Model χ^2)	*(46)*	*(60)*	*(63)*

*IMT, intima–media thickness. Values represent odds ratios (95% confidence intervals), *p<0.05.*

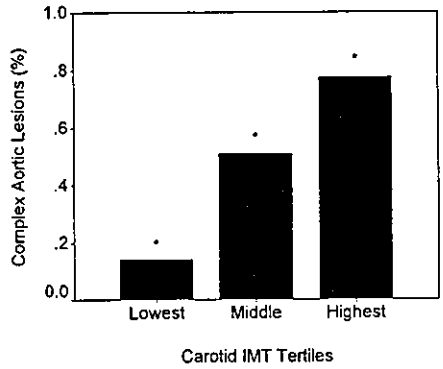

Fig 2. Frequency of complex aortic lesions by carotid intima–media thickness (IMT) tertiles. Complex aortic lesions are defined as mobile plaques, ulcers and/or intima–media thickness ≥4 mm. *p<0.05 compared with the lefthand adjacent tertile.

Additionally, there was a stepwise increase in the frequency of complex aortic lesions across the carotid IMT tertiles (Fig 2). In particular, complex aortic lesions were found in 38 of 49 (78%) patients in the highest tertile, compared with 7 of 49 (14%) patients in the lowest (p<0.05).

Discussion

We have shown an association between aortic and carotid atherosclerosis in ICVD, demonstrating the value of carotid evaluation for the identification of aortic lesions that are a potential ICVD risk.

Although both aortic and carotid atherosclerosis has been linked to a variety of cardiovascular risk factors, the factors predisposing to the pathology of the 2 arterial beds have not been clearly separated. In the current study, both aortic and carotid IMT increased with age, were greater in men, and appeared to have associations with traditional cardiovascular risk factors (Table 2), which has been shown elsewhere? Although hypertension had an independent association with carotid IMT, its association with aortic IMT was not significant when controlling for other risk factors. Based on this finding, hypertension has a stronger atherogenic effects on the carotid arteries than on the aortic arch;

however, our statistical power was limited, requiring much larger studies with refined criteria to establish this finding.

Despite the frequent coexistence of carotid stenosis in patients with aortic atherosclerosis[7,8] whether carotid findings can be used to stratify the severity of aortic atherosclerosis has not been established for ICVD. In the current study, we found a moderate linear relationship between aortic and carotid IMT (Fig 1), suggesting a link between aortic and carotid atherosclerosis. Moreover, the association was independent of age, sex and traditional cardiovascular risk factors (Table 3), further suggesting a linkage. In addition to carotid IMT, older age and smoking habit were independently associated with greater aortic IMT, supporting the study by Tribouilloy et al[10] Based on this result, older smokers with carotid atherosclerosis are more likely to have aortic arch atherosclerosis.

Kallikazaros et al have shown that carotid atheroma is predictive of aortic atheroma in cardiac patients[6] However, whether carotid lesions are predictive of aortic lesions that are a potential risk has not been fully established. Based on studies to date, complex aortic lesions, such as mobile plaques, ulcers and increased aortic IMT, are a greater risk for cerebral embolism[4,5] In the current study, each 1 SD increase in carotid IMT was associated with 4.2-fold higher likelihood for complex aortic lesions (Table 4). Moreover, the likelihood was only slightly affected by age, sex and other cardiovascular risk factors. These findings suggest the value of carotid evaluation for the identification of the potential risk of aortic lesions. Because age was another predictor for such lesions independent of carotid IMT, such a prediction would be more robust in older individuals with greater carotid IMT.

Additionally, it would be of clinical value to stratify the prevalence of complex aortic lesions by the carotid findings. The frequency of complex lesions increased in a stepwise fashion across the carotid IMT tertiles (Fig 2). Of note, complex aortic lesions were found in 78% of patients in the highest tertile, compared with 14% of those in the lowest. Based on this finding, the existence of an aortic source of emboli also needs to be considered when ICVD patients have increased carotid IMT. If such patients had embolic episodes of unknown origin, TEE would be the most effective modality for the exploration of ICVD etiology, with an additional caution for the observation of the aortic arch. Nonetheless, a considerable portion of the patients with less advanced carotid atherosclerosis had complex aortic lesions. Taken together, the severity of carotid atherosclerosis cannot be used as a definitive diagnostic marker for complex aortic lesions, but it can be a risk indicator for such lesions, potentially extending the benefit of routine carotid examination.

In patients with carotid atherosclerosis, silent cerebral infarction is often found not only in the ipsilateral, but also in the contralateral hemisphere[11,12] Given the association between aortic and carotid atherosclerosis, involvement of aortic lesions may need to be considered in the etiology of such infarction. Moreover, aortogenic cerebral embolism, whether symptomatic or asymptomatic, can occur during coronary or cerebral arteriography, and other aortic manipulations[13–15] Based on our findings, carotid evaluation prior to the procedures may help in the assessment of procedure-related risk for cerebral embolism, when TEE is not available.

Study Limitations

First, all patients in this study had been referred for clarification of ICVD etiology, implying a potential bias in patient selection. For example, patients with only deep, small infarctions were less likely to be referred, precluding a generalization of the findings to all ICVD patients. Nonetheless, TEE is most often considered for patients with indeterminate ICVD etiology, which supports the clinical value of our findings. Second, we defined complex aortic lesions from existing evidence[4,5] but the strength of their association with ICVD etiology is not established, requiring further studies to validate that definition.

Conclusion

In patients with ICVD, carotid atherosclerosis is associated with aortic atherosclerosis, which represents a risk factor for aortic lesions that are a potential ICVD risk. Noninvasive carotid evaluation prior to TEE may aid in determining the existence of such aortic lesions.

Acknowledgments

This study was supported in part by the research grants for cardiovascular diseases funded by the Ministry of Health, Labour and Welfare, and by the Smoking Research Foundation of Japan.

References

1. Amarenco P, Cohen A, Baudrimont M, Bousser MG. Transesophageal echocardiographic detection of aortic arch disease in patients with cerebral infarction. *Stroke* 1992; **23:** 1005–1009.
2. Jones EF, Kalman JM, Calafiore P, Tonkin AM, Donnan GA. Proximal aortic atheroma: An independent risk factor for cerebral ischemia. *Stroke* 1995; **26:** 218–224.
3. Toyoda K, Yasaka M, Nagata S, Yamaguchi T. Aortogenic embolic stroke: A transesophageal echocardiographic approach. *Stroke* 1992; **23:** 1056–1061.
4. Amarenco P, Cohen A, Tzourio C, Bertrand B, Hommel M, Besson G, et al. Atherosclerotic disease of the aortic arch and the risk of ischemic stroke. *N Engl J Med* 1994; **331:** 1474–1479.
5. The French Study of Aortic Plaques in Stroke Group. Atherosclerotic disease of the aortic arch as a risk factor for recurrent ischemic stroke: The French Study of Aortic Plaques in Stroke Group. *N Engl J Med* 1996; **334:** 1216–1221.
6. Kallikazaros IE, Tsioufis CP, Stefanadis CI, Pitsavos CE, Toutouzas PK. Closed relation between carotid and ascending aortic atherosclerosis in cardiac patients. *Circulation* 2000; **102:** III-263–III-268.
7. Demopoulos LA, Tunick PA, Bernstein NE, Perez JL, Kronzon I. Protruding atheromas of the aortic arch in symptomatic patients with carotid artery disease. *Am Heart J* 1995; **129:** 40–44.
8. Arko FR, Fritcher S, Mettauer M, Patterson DE, Buckley CJ, Manning LG. Mobile atheroma of the aortic arch and the risk of carotid artery disease. *Am J Surg* 1999; **178:** 206–208.
9. Uechi Y, Sunagawa O, Ishikawa N, Inoue T, Tamashiro M, Kamiyama T, et al. Risk factors for stiffness of the wall of the thoracic aorta in patients with mild atherosis. *Jpn Circ J* 2001; **65:** 409–413.
10. Tribouilloy C, Peltier M, Andrejak M, Rey JL, Lesbre JP. Correlation of thoracic aortic atherosclerotic plaque detected by multiplane transesophageal echocardiography and cardiovascular risk factors. *Am J Cardiol* 1998; **82:** 1552–1555, A8.
11. Brott T, Tomsick T, Feinberg W, Johnson C, Biller J, Broderick J, et al. Baseline silent cerebral infarction in the Asymptomatic Carotid Atherosclerosis Study. *Stroke* 1994; **25:** 1122–1129.
12. Hougaku H, Matsumoto M, Handa N, Maeda H, Itoh T, Tsukamoto Y, et al. Asymptomatic carotid lesions and silent cerebral infarction. *Stroke* 1994; **25:** 566–570.
13. Shmuely H, Zoldan J, Sagie A, Maimon S, Pitlik S. Acute stroke after coronary angiography associated with protruding mobile thoracic aortic atheromas. *Neurology* 1997; **49:** 1689–1691.
14. Bladin CF, Bingham L, Grigg L, Yapanis AG, Gerraty R, Davis SM. Transcranial Doppler detection of microemboli during percutaneous transluminal coronary angioplasty. *Stroke* 1998; **29:** 2367–2370.
15. Hamano K, Ikeda Y, Mikamo A, Okada H, Gohra H, Zempo N, et al. Atheromatous plaque in the distal aortic arch creating the potential for cerebral embolism during cardiopulmonary bypass. *Jpn Circ J* 2001; **65:** 161–164.

Journal of Neuroscience Research 72:461–471 (2003)

Implication of Cyclooxygenase-2 on Enhanced Proliferation of Neural Progenitor Cells in the Adult Mouse Hippocampus After Ischemia

Tsutomu Sasaki,[1]* Kazuo Kitagawa,[1] Shiro Sugiura,[1] Emi Omura-Matsuoka,[1] Shigeru Tanaka,[1] Yoshiki Yagita,[1] Hideyuki Okano,[3] Masayasu Matsumoto,[2] and Masatsugu Hori[1]

[1]Division of Strokology, Department of Internal Medicine and Therapeutics, Osaka University Graduate School of Medicine, Osaka, Japan
[2]Department of Clinical Neuroscience and Therapeutics, Division of Integrated Medical Science Programs for Biomedical Research, Hiroshima University Graduate School of Biomedical Sciences, Hiroshima, Japan
[3]Department of Physiology, Keio University Graduate School of Medicine, Tokyo, Japan

Global ischemia promotes neurogenesis in the dentate gyrus of the adult mouse hippocampus. Cyclooxygenase (COX)-2, the principal isoenzyme in the brain, modulates inflammation, glutamate-mediated cytotoxicity, and synaptic plasticity. We demonstrated that delayed treatment with different classes of COX inhibitor significantly blunted enhancement of dentate gyrus proliferation of neural progenitor cells after ischemia. COX-2 immunoreactivity was observed in both neurons and astrocytes in the dentate gyrus, but not in neural progenitor cells in the subgranular zone. Moreover, in the postischemic dentate gyrus of heterozygous and homozygous COX-2 knockout mice, proliferating bromodeoxyuridine-positive cells were significantly fewer than in wild-type littermates. These results demonstrate that COX-2 is an important modulator in enhancement of proliferation of neural progenitor cells after ischemia. © 2003 Wiley-Liss, Inc.

Key words: neurogenesis; hippocampus; COX-2; neuronal progenitor; musashi-1

In the subgranular zone (SGZ) of the dentate gyrus of the hippocampus and subventricular zone (SVZ) of the lateral ventricles, progenitor cells generate new neurons throughout adulthood. Ischemic insults to the brain have been shown to promote hippocampal neurogenesis in adult gerbils and rats (Liu et al., 1998; Jin et al., 2001; Yagita et al., 2001; Zhang et al., 2001; Iwai et al., 2002; Takasawa et al., 2002). Although, fibroblast growth factor-2 (FGF-2) and glutamate have been proposed to be involved in hippocampal neurogenesis after ischemia (Bernabeu and Sharp, 2000; Arvidsson et al., 2001; Yoshimura et al., 2001; Nakatomi et al., 2002), the molecular and cellular mechanisms underlying postischemic enhancement of neurogenesis remain unclear.

Cyclooxygenase (COX), a rate-limiting enzyme in synthesis of prostaglandins (PGs) from arachidonic acid, produces PGH2, which in subsequent steps gives rise to PGs with varied physiologic functions (Hayaishi, 1991; Smith et al., 1996; Kaufmann et al., 1997). Two Cox isoenzymes exist, COX-1 and COX-2, and COX-2 is expressed constitutively at relatively high levels in brain and kidney (Yamagata et al., 1993). In addition to the role of COX-2 in proinflammatory actions in the central nervous system (CNS), recent studies have found COX-2 to be a multifunctional neural modulator affecting synaptic plasticity (Kaufmann et al., 1996; Bazan, 2001) and glutamate-mediated cytotoxicity (Nogawa et al., 1997; Iadecola et al., 2001b). COX-2 also acts importantly in cell proliferation and has been implicated in growth and progression of a variety of tumor types (Tsujii et al., 1998; Shono et al., 2001).

Evidence is accumulating that quantities of circulating adrenal steroids negatively regulate neurogenesis in the dentate gyrus throughout life (Cameron and Gould, 1994; Gould and Cameron, 1996; Cameron and McKay, 1999) Glucocorticoids selectively inhibit expression of COX-2 without affecting COX-1. Thus, to determine whether COX-2 influences hippocampal neurogenesis in adult mice, we examined postischemic proliferation of progenitor cells in the SGZ after administering COX inhibitors with various specificities and postischemic neurogenesis in

Contract grant sponsor: Grant-in-aid for Scientific Research in Japan; Contract grant sponsor: The Takeda Science Foundation.

*Correspondence to: Tsutomu Sasaki, Division of Strokology, Department of Internal Medicine and Therapeutics (A8), Osaka University Graduate School of Medicine, 2-2 Yamadaoka, Suita City, Osaka 565-0871, Japan. E-mail: sasaki@medone.med.osaka-u.ac.jp

Received 22 October 2002; Revised 8 January 2003; Accepted 24 January 2003

COX-2 knockout mice. Because only a few experimental studies have examined neurogenesis in forebrain ischemia (Takagi et al., 1999) and focal ischemia (Yoshimura et al., 2001) in mice, we established initially profiles of hippocampal neurogenesis after ischemic insults to the mouse forebrain (Kitagawa et al., 1998).

MATERIALS AND METHODS

Animals

Adult male C57Black/6 mice (11–12 weeks old) were used in this study. The experimental protocol was approved by the Institutional Animal Care and Use Committee of Osaka University Graduate School of Medicine. They were fed standard laboratory chow and had free access to water before and after all procedures. Animal care was given according to the guidelines of Animal Center of Osaka University Graduate School of Medicine.

Cyclooxygenase-2 knockout mice (Dinchuk et al., 1995) were obtained from Jackson laboratories (Bar Harbor, ME). Mice were backcrossed to C57Black/6 mice five to seven times, and were studied at age of 10–12 weeks. Experiments were carried out in age-matched littermates, including those homozygous for the knockout (−/−), heterozygous (+/−), and wild type (+/+). Genotypes of all COX-2 knockout mice were determined by PCR analysis.

Transient Forebrain Ischemia

General anesthesia was maintained with 1% halothane by means of an open facemask. A polyacrylamide column for measurement of cortical microperfusion by laser-Doppler flowmetry (LDF; Advanced Laser Flowmetry) was attached to the skull, 3 mm lateral to the bregma on the right side, with dental cement. Body and skull temperature were monitored and maintained at 36.5–37.5°C with a heat lamp and mat. Both common carotid arteries were occluded for 12 min with microaneurysm clips and then reperfused. As described previously, only mice that showed less than 13% of baseline control microperfusion during the first minute of occlusion were used in subsequent experiments (Kitagawa et al., 1998).

Bromodeoxyuridine Labeling Protocols

Bromodeoxyuridine (BrdU; Roche Diagnostics, Indianapolis, IN), a thymidine analogue, was used to label proliferating cells. In the first experiment, mice with no surgery (control), mice with sham ischemia, and mice with ischemia were injected intraperitoneally (i.p.) with BrdU (50 mg/kg) four times every 2 hr over 6 hr to conclude at 6 hr, or 3, 6, 9, 13, and 27 days after ischemia. The next day, mice were killed under deep pentobarbital anesthesia and their brains were immersion-fixed in methanol at 4°C overnight for quantification of BrdU-positive cells. In other mice, to evaluate the phenotype of postmitotic cells, we injected BrdU (50 mg/kg) i.p. 9 days after ischemia four times every 2 hr over 6 hr. These mice were killed at 1, 14, or 30 days after BrdU administration. Mice with no surgery underwent the same sequence of injections and were sacrificed at corresponding times as a control group. Mice were perfused transcardially with 4% paraformaldehyde (PFA), then brains were removed and fixed in 4% PFA at 4°C overnight.

In the second experiment, examining the effect of COX in cell proliferation after ischemia, both right and left common carotid arteries were occluded for 12 min as described above. Ischemic mice were divided randomly into three groups. Indomethacin (Cayman Chemical, Ann Arbor, MI; 10 mg/kg), NS-398, (Cayman Chemical; 20 mg/kg), or vehicle alone was given at 9:00 AM and 9:00 PM on Day 8, and at 9:00 AM on Day 9 after ischemia. NS-398 inhibits COX-2 1,000 times more potently than COX-1 (Masferrer et al., 1994; Reitz et al., 1994). We administered BrdU (50 mg/kg) i.p. four times every 2 hr for 6 hr, starting 2 hr after the last injection of each COX inhibitor.

In the third experiment, we subjected COX-2 knockout mice, including homozygous (−/−), heterozygous (+/−), and wild-type littermates, to ischemia and BrdU-labeling protocols above.

Immunohistochemistry

For quantification of BrdU-positive cells, each tissue block was dehydrated after fixation and embedded in paraffin. Tissue sections (4 μm) encompassing the dorsal hippocampus 1.9 mm caudal from the bregma were examined after staining with cresyl violet. The protocol of BrdU immunohistochemistry was described previously (Takasawa et al., 2002). In brief, each deparaffinized section was treated in 50% formamide and 2× saline-sodium citrate buffer (2× SSC), and then incubated in 2 N HCl. After washing, sections were incubated with a rat monoclonal anti-BrdU antibody, 1:100 (Harlan Sera-Labo, Loughborough, UK) at 4°C overnight. Sections were then washed, incubated with a biotinylated secondary antibody, washed, and incubated further with a streptavidin-biotin-peroxidase complex (Vector Laboratories, Burlingame, CA). The sections were reacted finally with 0.05% 3'3-diaminobenzidine in the presence of 0.01% H_2O_2.

For double immunofluorescence, free-floating sections (40 μm) were incubated with primary antibody diluted with TBS/0.1% Triton X-100 containing 1.5% normal serum at 4°C overnight. Other mice were used for examination with frozen sections to assess COX-2 immunoreactivity. The following primary antibodies were used for immunofluorescence; rat monoclonal anti-BrdU antibody, 1:100 (Harlan Sera-Labo); mouse monoclonal anti-BrdU antibody, 1:200 (Amersham, Piscataway, NJ); mouse monoclonal anti-NeuN antibody, 1:200 (Chemicon, Temecula, CA); mouse monoclonal anti-microtubule associated protein (MAP) 2 antibody, 1:100 (Sigma, St. Louis, MO); rabbit polyclonal anti-glial fibrillary acidic protein (GFAP) antibody, 1:200 (Sigma); mouse monoclonal anti-glial fibrillary acidic protein (GFAP) antibody, 1:200 (Sigma); goat polyclonal anti-doublecortin (DCX) antibody, 1:100 (Santa Cruz Biotechnology, Santa Cruz, CA); rat monoclonal anti-Musashi-1 (Msi-1) antibody (14H1) (Kaneko et al., 2000) 1:200; mouse monoclonal anti-β-tubulin III antibody, 1:200 (Chemicon); and rabbit polyclonal anti-COX-2 antibody, 1:200 (Cayman Chemical).

For double labeling of BrdU and cell markers (NeuN and MAP2 for mature neurons, β-tubulin III for immature neurons, GFAP for astrocytes, DCX for migrating neuroblasts and immature neurons, and Msi-1 for neuronal progenitors, neuronal stem cells, and astrocytes), sections were incubated with an anti-BrdU antibody plus an antibody for one of the above cell

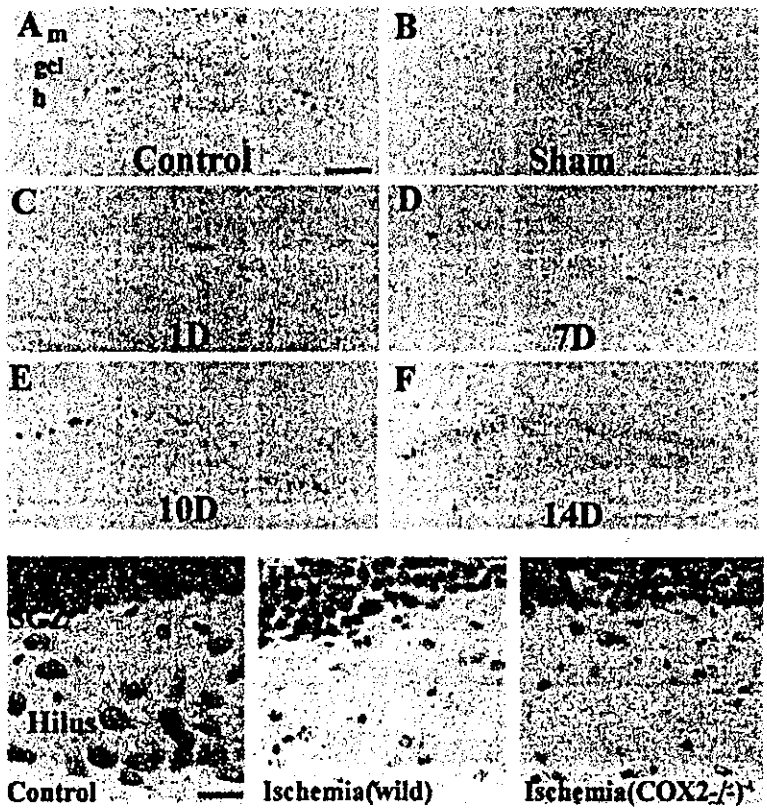

Fig. 1. Distribution of BrdU-positive cells in the mouse dentate gyrus after forebrain ischemia. BrdU (50 mg/kg, i.p.) was administered four times every 2 hr over 6 hr. Mice received BrdU concluding at 6 hr or 3, 6, 9, 13, or 27 days after ischemia (n = 6 in each group). On the next day mice were killed, and brains were processed for BrdU immunohistochemistry. Ischemia resulted in an increase of BrdU-positive proliferating cells in the subgranular zone (SGZ). Control (A), nonischemic sham (B), and ischemic mice killed 1 (C), 7 (D), 10 (E), and 14 (F) after ischemia. Neuronal damage was assessed histologically by Nissl staining (G–I). COX-2 knockout mice (I) showed a similar degree of neuronal loss in the dentate hilus as in wild-type littermates (H). Scale bars = 0.1 mm in A (applies to A–F); 50 μm in G (applies to G–I). [Color figure can be viewed in the online issue, which is available at www.interscience.wiley.com.]

markers at 4°C overnight after DNA denaturation, and then incubated with appropriate anti-IgG secondary donkey antibodies conjugated to fluorescein isothiocyanate (FITC) or rhodamine (Chemicon, 1:200) for 90 min at room temperature. After rinsing with Tris buffer, sections were mounted with Vectorshield (Vector Laboratories) and visualized or photographed with a confocal microscopy system (Zeiss LSM-410, Oberkochen, Germany).

Quantification

To count BrdU-labeled cells as identified by the immunoperoxidase reaction, five sections from the hippocampus were cut every 120 μm beginning 1.4 mm caudal and 1.9 mm caudal to the bregma. In the hippocampus, the granular cell layer (GCL, 50 μm) and SGZ, defined as a zone two cell bodies wide (5 μm) along the border of the GCL and hilus, were considered together for quantification. The mean density of BrdU-labeled cells in each mouse was calculated as the number of labeled nuclei divided by the area.

To assess the phenotype of BrdU-labeled cells after ischemia or sham ischemia in double immunofluorescence, we detected BrdU-positive cells in the SGZ and GCL, and then determined whether these cells expressed Msi-1, DCX, β-tubulin III, NeuN, MAP2, or GFAP. A mean value for each marker was obtained using 10 sections from five mice. Data in the text and figure are described as mean ± SD. Multiple comparisons were evaluated statistically by the analysis of variance, followed by Scheffe's post-hoc tests.

RESULTS

Cell Proliferation in the Mouse Hippocampus After Ischemia

A few BrdU-positive cells were observed in the SGZ of the hippocampal dentate gyrus in the control (Fig. 1A; 21.6 ± 10.7/mm^2, n = 10). The temporal and regional profiles of BrdU labeling in the SGZ did not differ significantly between nonischemic control mice and mice with sham ischemia (Fig. 1B; 18.9 ± 10.2/mm^2, n = 6). BrdU-positive cells exhibited a slight decrease 1 day after the ischemic insult (Fig. 1C; 11.2 ± 8.0/mm^2, n = 6). The number of BrdU-positive cells in the SGZ was increased at 4 days (51.5 ± 21.9/mm^2, n = 6), reached a peak at 7 and 10 days (Fig. 1D; 77.0 ± 33.3/mm^2, n = 6 and Fig. 1E; 98.7 ± 26.6/mm^2, n = 6, respectively), then declined by 14 days (Fig. 1F; 45.5 ± 22.1/mm^2, n = 6), and returned to the control levels by 28 days (20.4 ± 11.1/mm^2, n = 6) after ischemia. Semiquantitative analysis in the SGZ showed the number of BrdU-positive cells to be increased significantly compared to the control and sham groups by 4–5 times at 7 and 10 days after ischemia.

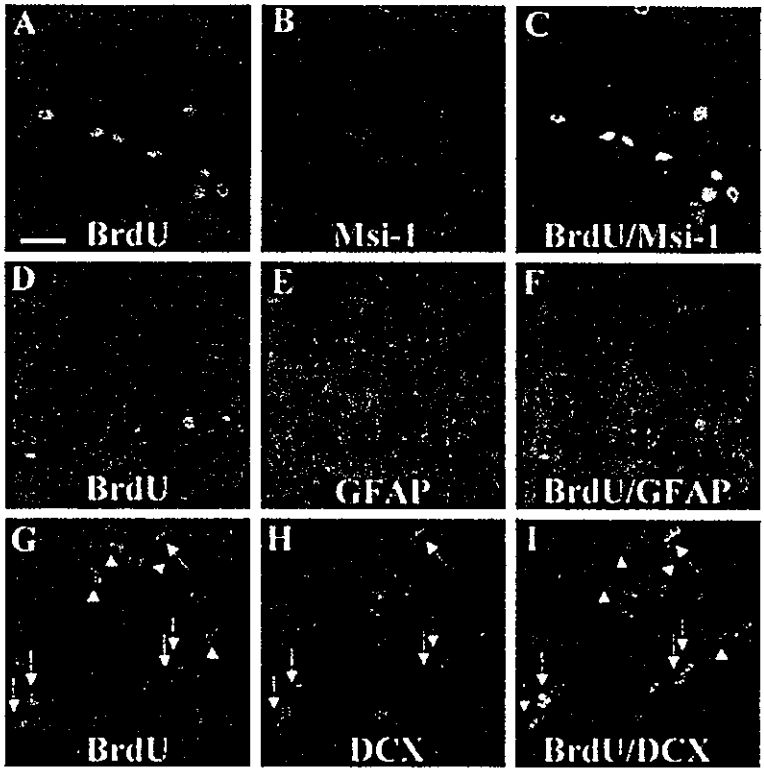

Fig. 2. Characterization of newly generated cells in the SGZ and GCL. To label new cells, mice received BrdU (50 mg/kg, i.p. administration) four times on Day 9 after ischemia. In the SGZ and GCL, double immunofluorescent staining shows BrdU-immunoreactive cells (A, D, G), and cells immunoreactive for Msi-1 (B), GFAP (E), or DCX (H). Merged images show BrdU/Msi-1 (C), BrdU/GFAP (F), and BrdU/DCX (I). Most BrdU-positive cells expressed Msi-1, but only a few expressed GFAP (D–F). About half of BrdU-positive cells expressed DCX. BrdU-plus-DCX-positive cells are indicated with arrows, whereas BrdU-positive, DCX-negative cells are shown with arrowheads (G–I). Scale bar = 50 μm.

TABLE I. BrdU-Positive Cells and the Characteristic Phenotype 1 Day After BrdU Administration in Ischemic and Nonischemic Control Mice

	Total BrdU(+) cells/mm^2	BrdU(+) Msi-1(+)/total BrdU(+) (%)	BrdU(+) GFAP(+)/total BrdU(+) (%)	BrdU(+) DCX(+)/total BrdU(+) (%)
Control	21.6 ± 10.7	94.7 ± 4.1	10.5 ± 5.4	55.8 ± 14.6
Ischemia	106.0 ± 21.1	95.8 ± 2.3	16.1 ± 6.9	48.8 ± 14.0

All mice subjected to ischemia showed neuronal loss in the hilus of the dentate gyrus (Fig. 1G–I).

Characteristics of Proliferating Cells in the Mouse Hippocampus After Ischemia

To determine the phenotype of BrdU-positive cells in the SGZ 1 day after BrdU administration, double immunofluorescence for BrdU/Msi-1, BrdU/GFAP, or BrdU/DCX was evaluated (Fig. 2). In both nonischemic controls and ischemic mice, most BrdU-positive cells in the SGZ coexpressed Msi-1 (94.7 ± 4.1% in control mice and 95.8 ± 2.3% in ischemic mice; Fig. 2A–C, Table I), whereas only 10–15% of BrdU-positive cells exhibited GFAP (10.5 ± 5.4% in control mice and 16.1 ± 6.9% in ischemic mice; Fig. 2D–F, Table I). Roughly half of BrdU-positive cells in the SGZ showed colocalization with DCX (55.8 ± 14.6% in control mice and 48.8 ± 14.0% in ischemic mice; Fig. 2G–I, Table I).

We examined further progenitor cell differentiation at 14 or 30 days after BrdU administration by double immunofluorescence for BrdU/β-tubulin III, BrdU/NeuN, BrdU/MAP2, or BrdU/GFAP. Most BrdU-positive cells exhibited neuronal phenotypes (Figs. 3 and 4). By semiquantitative analysis, more than 80% of BrdU-positive cells in the SGZ and GCL exhibited NeuN in both groups (83.6 ± 5.7% in control mice and 89.9 ± 4.0% in ischemic mice; Table II). In contrast, only 5–15% of BrdU-positive cells in the SGZ and GCL were colabeled with GFAP (12.6 ± 3.1% in control mice and 5.8 ± 4.7% in ischemic mice; Fig. 3, Table II).

Next, we examined whether these nascent BrdU-positive neurons could be integrated into neural circuits. New BrdU-positive granular cells expressing the mature neuronal marker MAP2 extended the dendritic processes toward and into the molecular layer (Fig. 4A–F).

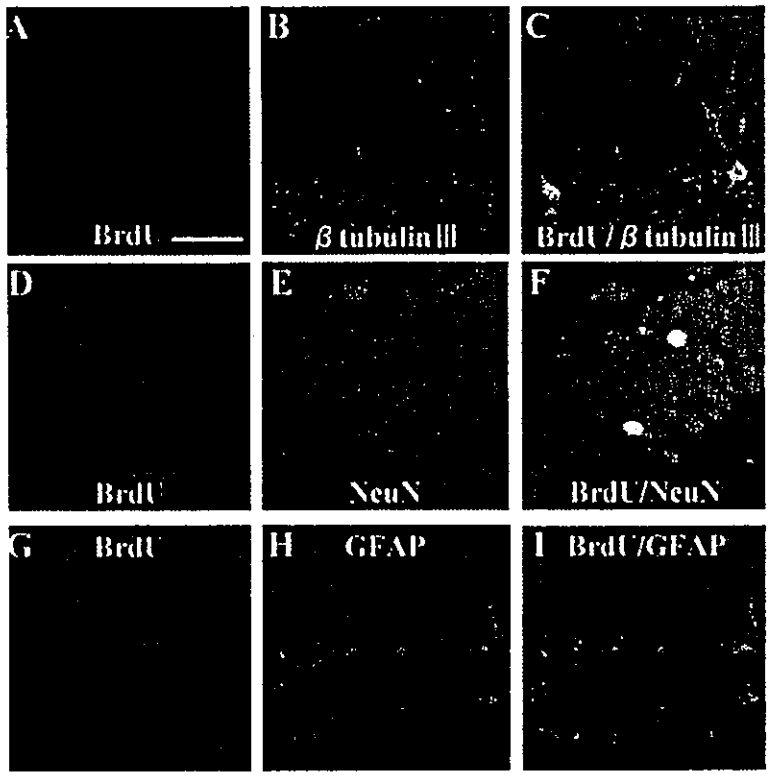

Fig. 3. Neuronal differentiation of newly formed cells in the SGZ and GCL after ischemia. BrdU (50 mg/kg, i.p.) was administered 9 days after ischemia, and mice were killed 14 (A–C) or 30 days (D–I) after BrdU administration. At 14 days after BrdU administration, most BrdU-positive cells expressed immunoreactive β-tubulin III (A–C). At 30 days after BrdU administration, most BrdU-positive cells expressed NeuN (D–F). In contrast, few BrdU-positive cells exhibited GFAP immunoreactivity in the SGZ and GCL (G–I). Scale bar = 40 μm.

TABLE II. Differentiation into Neuron and Astrocyte and Survival 30 Days after BrdU Administration in Ischemic and Nonischemic Control Mice

	Total BrdU(+) cells/mm^2	BrdU(+) NeuN(+)/total BrdU(+) (%)	BrdU(+) GFAP(+)/total BrdU(+) (%)
Control	4.7 ± 4.8	83.6 ± 5.7	12.6 ± 3.1
Ischemia	38.7 ± 13.1	89.9 ± 4.0	5.8 ± 4.7

COX-2 Expression in the Mouse Hippocampus

In control animals, COX-2 immunoreactive neurons were found in the CA4 sectors and the dentate gyrus (Fig. 5A–C). At 10 days after ischemia, the level of neuronal COX-2 immunoreactivity was almost the same as basal expression in dentate gyrus granular cells (Fig. 5D–I). Consistent with the previous finding that COX2 was localized in nuclear envelope and endoplasmic reticulum (Morita et al., 1995), COX-2 immunoreactivity in the neuron was observed in the perinuclear region in either control or 10 days after ischemia (Fig. 5A–I). Notably, COX-2 immunoreactivity was expressed in GFAP-positive hypertrophic reactive astrocytes in the hilus after ischemia (Fig. 5D–F), but not in control animals (Fig. 5A–C).

BrdU-positive cells in the SGZ did not express COX-2 in control or ischemic mice on the next day after BrdU administration (Fig. 6A –C). In addition, Msi-1-positive cells in the SGZ did not coexpress COX-2 (Fig. 6D–F). Thus, we concluded that the Msi-1- and BrdU-positive neuronal progenitors in the SGZ did not express COX-2.

COX Inhibitor Decreased the Proliferation of Progenitor Cells in SGZ after Ischemia

In nonischemic control mice, the number of BrdU-positive cells in vehicle, indomethacin, and NS-398 treated groups were 16.3 ± 10.5, 11.8 ± 5.7, and 13.7 ± 8.1/mm^2, respectively, (Fig. 7A, n = 6 mice in each group). In the ischemic group, mice treated with indomethacin and NS-398 showed a significant decrease in the number of BrdU-positive cells in the SGZ compared to vehicle-treated mice at 10 days after ischemia (56.0 ± 30.3/mm^2 in mice treated with vehicle, 35.6 ± 22.0/mm^2 in mice treated with indomethacin, and 34.2 ± 25.8/mm^2 in mice treated with NS-398; Fig. 7A, n = 6 mice in each group).

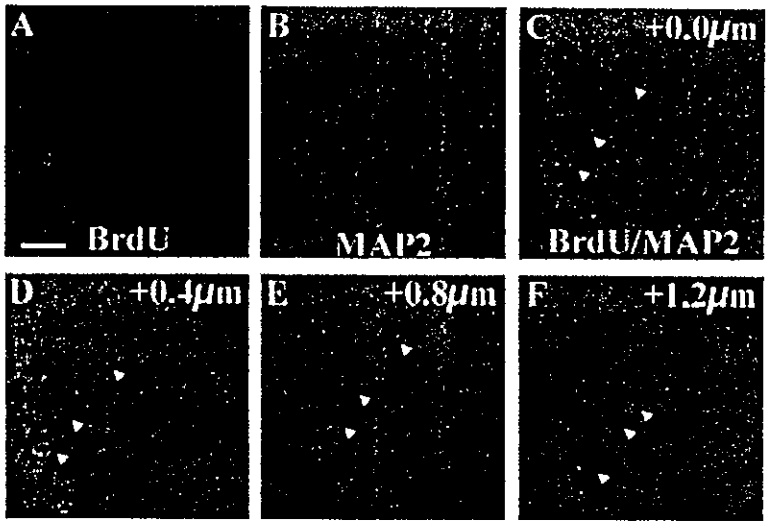

Fig. 4. New neurons extended dendritic processes. At 30 days after BrdU administration, BrdU-positive cells expressed MAP2 immunoreactivities (**A–C**). Z-series analysis (**D–F**) indicated that new cells colabeled with BrdU and MAP2 extended dendritic processes toward and into the molecular layer. Scale bar = 75 μm.

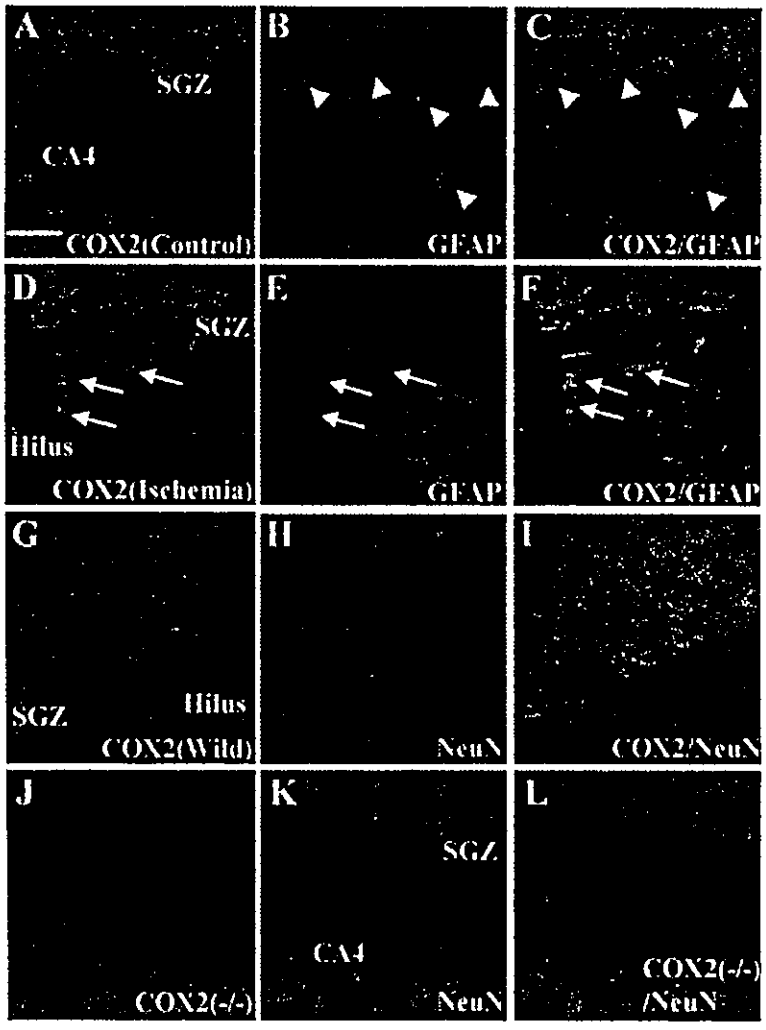

Fig. 5. COX-2 expression was demonstrated in neurons and reactive astrocytes, and not induced in COX-2 knockout mice. Presence or absence of COX-2 immunoreactivity is shown in neurons and astrocytes in the SGZ and hilus in control and 10 days after ischemia. BrdU was administered in controls and 9 days after ischemia. In control mice, COX-2 immunoreactivity was not expressed in astrocytes in the SGZ and hilus as indicated with arrowheads (**A–C**). On the other hand, in ischemic mice, COX-2 immunoreactivity was demonstrated in GFAP-positive hypertrophic reactive astrocytes as indicated with arrows (**D–F**) in addition to neurons (**G–I**). COX-2 immunoreactivity was not detected in COX-2 knockout mice (**J–L**). Merged images show (C,F) COX-2/GFAP and (I,L) COX-2/NeuN. Scale bar = 40 μm.

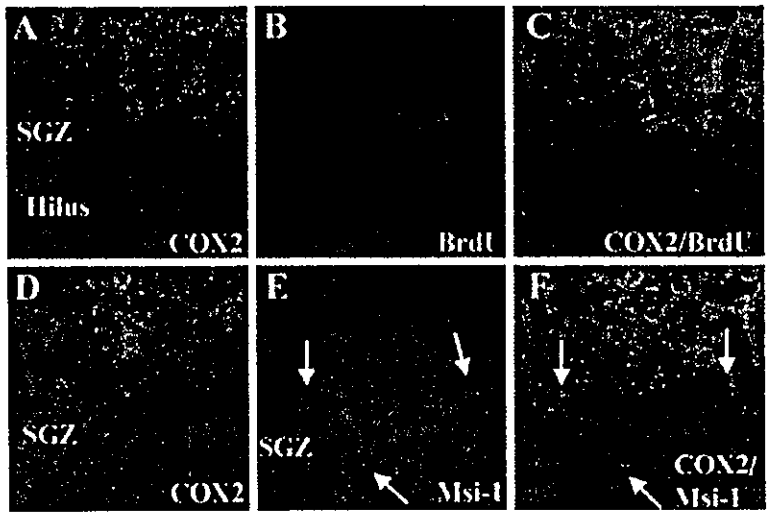

Fig. 6. COX-2 expression was not observed in neural progenitor cells. BrdU was administered 9 days after ischemia. Merged image (C) shows COX-2/BrdU; (F), COX-2/Msi-1. COX-2 immunoreactivity was not detected in BrdU-positive proliferating progenitor cells (A–C) nor in Msi-1-positive cells in the SGZ (D–F). Msi-1-positive, COX-2-negative cells are shown with arrows (D–F). Scale bar = 40 μm.

Progenitor Cells Proliferation in COX-2 Knockout Mice After Ischemia

In COX-2 knockout mice, COX-2 immunoreactivity was not observed in the control or in the ischemic hippocampus (Fig. 5J–L). In all COX-2 knockout mice subjected to ischemia, neuronal loss in the dentate hilus was observed similarly (Fig. 1I). In nonischemic control mice, numbers of BrdU-positive cells in the SGZ of COX-2 +/+, +/−, and −/− mice were 23.3 ± 8.7/mm^2, 17.7 ± 7.5/mm^2, and 14.5 ± 6.2/mm^2, respectively (Fig. 7B).

In the ischemic groups, BrdU-positive cells in the SGZ 10 days after ischemia in COX-2 +/+ mice were significantly more numerous (79.6 ± 32.5/mm^2) than in COX-2 +/+ nonischemic control mice (about 3.5 times). Numbers of BrdU-positive cells after ischemic insults were significantly less in COX-2 +/− (48.3 ± 24.6/mm^2) and COX-2 −/− mice (39.3 ± 21.2/mm^2) than in COX-2 +/+ mice (Fig. 7B).

DISCUSSION

Our data demonstrated that transient forebrain ischemia increased neurogenesis in the dentate gyrus of the adult mouse hippocampus. The postischemic enhanced proliferation of neural progenitor cells in the SGZ was attenuated by COX inhibitors and in COX-2 knockout mice.

Increased Neurogenesis by Progenitor Cells in the Ischemic Mouse Hippocampus

Consistent with previous reports using a global ischemia model (Liu et al., 1998; Takagi et al., 1999; Yagita et al., 2001), the number of BrdU-positive cells in the SGZ peaked 10 days after ischemia. On the day after BrdU injection, most BrdU-positive cells in the SGZ also expressed Msi-1, and about half of those cells exhibited DCX; however, only about 10% of BrdU-positive cells coexpressed GFAP. Msi-1 is highly enriched in neural progenitor/stem cells and astrocytes (Sakakibara et al., 1996; Sakakibara and Okano, 1997; Kaneko et al., 2000). In the present study, BrdU- and Msi-1-positive but GFAP-negative cells were identified as neural progenitor cells (Yagita et al., 2001; Takasawa et al., 2002). A recent report, however, suggested that GFAP-positive astrocytes in the SGZ generated new neurons via GFAP-negative intermediate neuronal progenitor cells in the adult mammalian hippocampus (Seri et al., 2001). Because conversion to the GFAP-negative intermediate progenitors was rapid (Seri et al., 2001), many of the BrdU-positive cells were already GFAP-negative 24 hr after BrdU administration in the present study. Because recent experiments using both neurosphere and a monolayer culture method suggested that the adult dentate gyrus did not contain resident neural stem cells (Seaberg and van der Kooy, 2002), the progenitor or stem cells in the SGZ, therefore, must be identified carefully. DCX is a neural microtubule-associated protein associated with neuronal migration that is expressed in both migrating neuroblasts and immature neurons (Francis et al., 1999; Gleeson et al., 1999; Gu et al., 2000; Jin et al., 2001). Our results suggested that DCX also was expressed by a subset of neural lineage cells derived from Msi-1-positive neural progenitor cells in the ischemic hippocampus.

Newborn Neurons After Ischemic Insult Extend Dendrites

Newly generated neurons in the dentate gyrus of the adult hippocampus have been reported to send appropriate axonal projections to the CA3 sector under physiologic conditions (Markakis and Gage, 1999), and also after seizures (Parent et al., 1997). The newly generated neurons were integrated functionally into the hippocampal circuitry according to retroviral labeling (van Praag et al., 2002); however, whether cells newly generated in the SGZ after ischemic insult became functional remained unknown. We showed that BrdU- and MAP2-positive

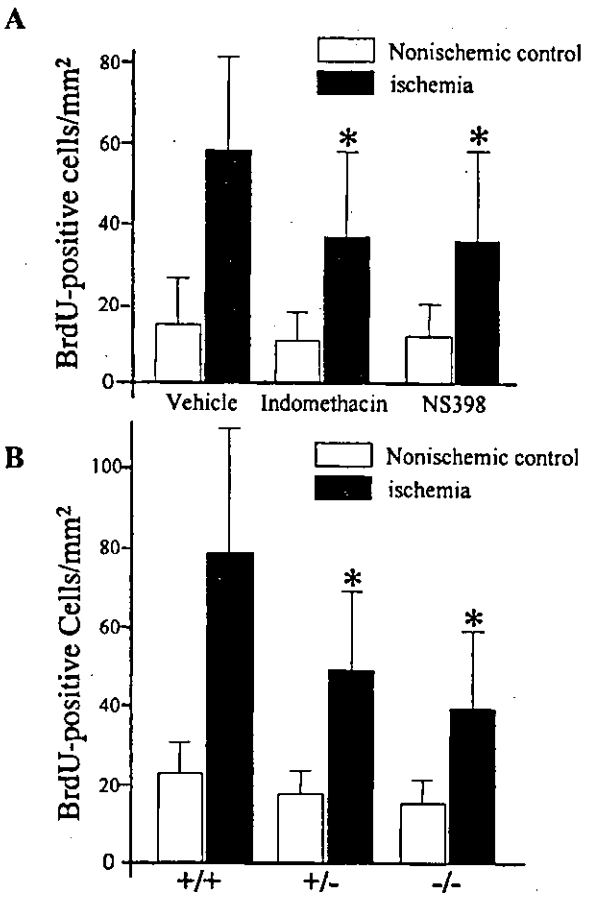

Fig. 7. Treatment with COX inhibitors or COX-2 knockout mice blunted the proliferation of progenitor cells after ischemia. Numbers of BrdU-positive cells in the SGZ are shown in nonischemic control and in ischemic mice after treatment with vehicle, indomethacin, or NS-398 **A:** Mice received BrdU (50 mg/kg, i.p.) four times every 2 hr for 6 hr starting 2 hr after the last COX inhibitor injection. They were killed 24 hr after the last BrdU administration. In contrast to the number of BrdU-positive cells in nonischemic controls (open bars), in ischemic mice (filled bars), the number of BrdU-positive cells in groups with indomethacin or NS-398 treatment in the SGZ was decreased significantly compared to vehicle treatment (n = 6 mice in each group). **B:** The number of BrdU-positive cells in controls and after ischemia in COX-2 +/+, +/−, and −/− knockout mice. In controls (open bars), the number of BrdU-positive cells in the SGZ in COX +/− (n = 6) or COX −/− (n = 4) mice were slightly less than in COX +/+ mice (n = 5), but the difference was not significant. In ischemic group (filled bars), the number of BrdU-positive cells after ischemia was significantly less in COX +/− (n = 6) or COX −/− mice (n = 5) than in COX +/+ (n = 6) mice. Data are the mean ± SD. The significance of differences was determined using ANOVA followed by Scheffe's post hoc tests. *$P < 0.05$ compared to control group.

newborn cells extended dendritic processes toward and into the molecular layer (Fig. 4). These findings indicated that, whereas cell proliferation in the dentate gyrus after an ischemic insult was transient, the resulting new neurons could be integrated into neural circuits.

COX-2 Is Expressed in Neurons and Reactive Astrocytes, But Not in Neural Progenitor Cells

In pathologic conditions, COX-2 has been shown to be induced after seizures (Yamagata et al., 1993), spreading depression (Miettinen et al., 1997), and ischemia (Nogawa et al., 1997; Iadecola et al., 2001b), and therefore may contribute to neuronal injury after brain ischemia. COX-2 mRNA and protein are upregulated immediately after either global (Ohtsuki et al., 1996; Koistinaho et al., 1999) or focal ischemia (Collaco-Moraes et al., 1996). Furthermore, prolonged COX-2 expression was observed in vulnerable neurons after global ischemia (Koistinaho et al., 1999; Matsuoka et al., 1999), and in neurons of the ischemic penumbra region after middle cerebral artery occlusion (Nogawa et al., 1997). In addition to neuronal localization, we also showed COX-2 immunoreactivity in reactive astrocytes, but not in astrocytes in control mice, in the hilus of the ischemic hippocampus, as reported previously (Degi et al., 1998; Sandhya et al., 1998; Hirst et al., 1999). Song et al. (2002) demonstrated recently that both neonatal and adult astrocytes in the hippocampus induced neurogenesis from neural stem cells. Therefore, it is also possible that COX-2 expression in astrocytes is important for the neurogenesis-inducing actions of these cells. COX-2 has been shown to be involved with cell cycle activity (Hoozemans et al., 2002; Mirjany et al., 2002). As mitotic proliferation is a critical component in adult neurogenesis, we initially estimated that neural progenitor cells themselves might express COX-2 at certain stages in their proliferation and differentiation; however, we could not detect COX-2 immunoreactivity in neural progenitors in the SGZ. Based on these findings, COX-2 in neurons and reactive astrocytes of the dentate gyrus is highly likely to be an important modulator inducing proliferation of progenitor cells in the SGZ after ischemia.

Involvement of COX-2 in Postischemic Proliferation of Neural Progenitors in the Hippocampus

In this study, enhanced proliferation of neural progenitor cells after ischemia was attenuated by treatment with COX inhibitors, and in COX-2 knockout mice. Although the suppression of enhanced neurogenesis after ischemia by administration of acetylsalicylic acid already has been reported (Kumihashi et al., 2001), acetylsalicylic acid has other COX-independent effects, such as inhibition of nuclear factor (NF) -κB, in addition to inhibiting COX (Yin et al., 1998). Therefore, our study demonstrated for the first time the involvement of COX-2 in ischemia-induced neurogenesis, although the differentiation of neural progenitor cells under COX-2 inhibition requires future clarification. The effect of the nonselective COX inhibitor indomethacin on postischemic proliferation of neural progenitor cells in the SGZ was almost the same as selective COX-2 inhibitor NS-398. This finding indicated that COX-1 as well as COX-2 might affect neural progenitor cells proliferation after ischemia. Although the role of COX-1 in ischemic brain injury has

been controversial (Iadecola et al., 2001a), it has been suggested that prostaglandin and prostacyclin produced by COX-1 play a crucial role in brain ischemia (Lin et al., 2002). Therefore, further studies are needed to determine whether COX-1 influence postischemic proliferation of neural progenitor cells.

COX-2 may affect neurogenesis in the dentate gyrus at least partly through generation of PGs, particularly PGE2, via the intermediate PGH2. It has been suggested that astrocytes could synthesize and release significant amounts of prostaglandins in vitro (Hirst et al., 1999). A recent study demonstrated that PGE2 transactivated a receptor for epidermal growth factor (EGF) and triggered mitogenic signaling (Pai et al., 2002). Multiple growth factors, including FGF-2 (Kuhn et al., 1997), EGF (Reynolds and Weiss, 1992), brain derived neurotrophic factor (BDNF) (Ahmed et al., 1995), and insulin-like growth factor (IGF) (Arsenijevic and Weiss, 1998), are known to be important regulators of proliferation and differentiation in neural stem cells. EGF receptor-like immunoreactivity was detected in proliferating cells in the dentate gyrus (Okano et al., 1996). Involvement of FGF-2 in hippocampal neurogenesis after ischemia already has been demonstrated. Involvement of FGF-2 in hippocampal neurogenesis after ischemia already has been demonstrated (Yoshimura et al., 2001). Additionally, PGE2 induced IL-6 release in astrocytes (Fiebich et al., 2001). The role of growth factors or IL-6 in neurogenesis has been already elucidated (Yoshimura et al., 2001; Vallieres et al., 2002). Interestingly, the microinjections of prostaglandin F2α (PGF2α) induced delayed VEGF expression (Skold et al., 2000). Moreover, VEGF receptor Flk-1 has been reported recently to be expressed in BrdU- and DCX-labeled immature neurons in the SGZ and SVZ (Jin et al., 2002). Based on these findings, COX-2 may influence neurogenesis in the dentate gyrus through the modulation of prostaglandin-mediated factors.

In summary, our study provides evidence that COX-2 is an important regulator in hippocampal neurogenesis in the dentate gyrus after ischemic insults. In addition, COX-2 immunoreactivity was observed in both neurons and astrocytes in the dentate gyrus, but not in neural progenitor cells in the subgranular zone. Elucidation of molecular pathways via COX-2 that underlie enhancement of neurogenesis after ischemia would be important for the therapeutic application of enhanced neurogenesis in stroke patients.

ACKNOWLEDGMENTS

This study was supported by a Grant-in-Aid for Scientific Research (B) and (C) in Japan and by Takeda Science Foundation. We thank R. Morimoto and S. Imoto for secretarial assistance.

REFERENCES

Ahmed S, Reynolds BA, Weiss S. 1995. BDNF enhances the differentiation but not the survival of CNS stem cell-derived neuronal precursors. J Neurosci 15:5765–5778.

Arsenijevic Y, Weiss S. 1998. Insulin-like growth factor-I is a differentiation factor for postmitotic CNS stem cell-derived neuronal precursors: distinct actions from those of brain-derived neurotrophic factor. J Neurosci 18:2118–2128.

Arvidsson A, Kokaia Z, Lindvall O. 2001. *N*-methyl-D-aspartate receptor-mediated increase of neurogenesis in adult rat dentate gyrus following stroke. Eur J Neurosci 14:10–18.

Bazan NG. 2001. COX-2 as a multifunctional neuronal modulator. Nat Med 7:414–415.

Bernabeu R, Sharp FR. 2000. NMDA and AMPA/kainate glutamate receptors modulate dentate neurogenesis and CA3 synapsin-I in normal and ischemic hippocampus. J Cereb Blood Flow Metab 20:1669–1680.

Cameron HA, Gould E. 1994. Adult neurogenesis is regulated by adrenal steroids in the dentate gyrus. Neuroscience 61:203–209.

Cameron HA, McKay RD. 1999. Restoring production of hippocampal neurons in old age. Nat Neurosci 2:894–897.

Collaco-Moraes Y, Aspey B, Harrison M, de Belleroche J. 1996. Cyclo-oxygenase-2 messenger RNA induction in focal cerebral ischemia. J Cereb Blood Flow Metab 16:1366–1372.

Degi R, Bari F, Beasley TC, Thrikawala N, Thore C, Louis TM, Busija DW. 1998. Regional distribution of prostaglandin H synthase-2 and neuronal nitric oxide synthase in piglet brain. Pediatr Res 43:683–689.

Dinchuk JE, Car BD, Focht RJ, Johnston JJ, Jaffee BD, Covington MB, Contel NR, Eng VM, Collins RJ, Czerniak PM, et al. 1995. Renal abnormalities and an altered inflammatory response in mice lacking cyclooxygenase II. Nature 378:406–409.

Fiebich BL, Schleicher S, Spleiss O, Czygan M, Hull M. 2001. Mechanisms of prostaglandin E2-induced interleukin-6 release in astrocytes: possible involvement of EP4-like receptors, p38 mitogen-activated protein kinase and protein kinase C. J Neurochem 79:950–958.

Francis F, Koulakoff A, Boucher D, Chafey P, Schaar B, Vinet MC, Friocourt G, McDonnell N, Reiner O, Kahn A, McConnell SK, Berwald-Netter Y, Denoulet P, Chelly J. 1999. Doublecortin is a developmentally regulated, microtubule-associated protein expressed in migrating and differentiating neurons. Neuron 23:247–256.

Gleeson JG, Lin PT, Flanagan LA, Walsh CA. 1999. Doublecortin is a microtubule-associated protein and is expressed widely by migrating neurons. Neuron 23:257–271.

Gould E, Cameron HA. 1996. Regulation of neuronal birth, migration and death in the rat dentate gyrus. Dev Neurosci 18:22–35.

Gu W, Brannstrom T, Wester P. 2000. Cortical neurogenesis in adult rats after reversible photothrombotic stroke. J Cereb Blood Flow Metab 20:1166–1173.

Hayaishi O. 1991. Molecular mechanisms of sleep-wake regulation: roles of prostaglandins D2 and E2. FASEB J 5:2575–2581.

Hirst WD, Young KA, Newton R, Allport VC, Marriott DR, Wilkin GP. 1999. Expression of COX-2 by normal and reactive astrocytes in the adult rat central nervous system. Mol Cell Neurosci 13:57–68.

Hoozemans JJ, Bruckner MK, Rozemuller AJ, Veerhuis R, Eikelenboom P, Arendt T. 2002. Cyclin D1 and cyclin E are co-localized with cyclo-oxygenase 2 (COX-2) in pyramidal neurons in Alzheimer disease temporal cortex. J Neuropathol Exp Neurol 61:678–688.

Iadecola C, Niwa K, Nogawa S, Zhao X, Nagayama M, Araki E, Morham S, Ross ME. 2001b. Reduced susceptibility to ischemic brain injury and *N*-methyl-D-aspartate-mediated neurotoxicity in cyclooxygenase-2-deficient mice. Proc Natl Acad Sci USA 98:1294–1299.

Iadecola C, Sugimoto K, Niwa K, Kazama K, Ross ME. 2001a. Increased susceptibility to ischemic brain injury in cyclooxygenase-1-deficient mice. J Cereb Blood Flow Metab 21:1436–1441.

Iwai M, Sato K, Omori N, Nagano I, Manabe Y, Shoji M, Abe K. 2002. Three steps of neural stem cells development in gerbil dentate gyrus after transient ischemia. J Cereb Blood Flow Metab 22:411–419.

Jin K, Minami M, Lan JQ, Mao XO, Batteur S, Simon RP, Greenberg DA. 2001. Neurogenesis in dentate subgranular zone and rostral subventricular zone after focal cerebral ischemia in the rat. Proc Natl Acad Sci USA 98:4710–4715.

Jin K, Zhu Y, Sun Y, Mao XO, Xie L, Greenberg DA. 2002. Vascular endothelial growth factor (VEGF) stimulates neurogenesis in vitro and in vivo. Proc Natl Acad Sci USA 99:11946–11950.

Kaneko Y, Sakakibara S, Imai T, Suzuki A, Nakamura Y, Sawamoto K, Ogawa Y, Toyama Y, Miyata T, Okano H. 2000. Musashi1: an evolutionally conserved marker for CNS progenitor cells including neural stem cells. Dev Neurosci 22:139–153.

Kaufmann WE, Andreasson KI, Isakson PC, Worley PF. 1997. Cyclooxygenases and the central nervous system. Prostaglandins 54:601–624.

Kaufmann WE, Worley PF, Pegg J, Bremer M, Isakson P. 1996. COX-2, a synaptically induced enzyme, is expressed by excitatory neurons at postsynaptic sites in rat cerebral cortex. Proc Natl Acad Sci USA 93:2317–2321.

Kitagawa K, Matsumoto M, Yang G, Mabuchi T, Yagita Y, Hori M, Yanagihara T. 1998. Cerebral ischemia after bilateral carotid artery occlusion and intraluminal suture occlusion in mice: evaluation of the patency of the posterior communicating artery. J Cereb Blood Flow Metab 18:570–579.

Koistinaho J, Koponen S, Chan PH. 1999. Expression of cyclooxygenase-2 mRNA after global ischemia is regulated by AMPA receptors and glucocorticoids. Stroke 30:1900–1906.

Kuhn HG, Winkler J, Kempermann G, Thal LJ, Gage FH. 1997. Epidermal growth factor and fibroblast growth factor-2 have different effects on neural progenitors in the adult rat brain. J Neurosci 17:5820–5829.

Kumihashi K, Uchida K, Miyazaki H, Kobayashi J, Tsushima T, Machida T. 2001. Acetylsalicylic acid reduces ischemia-induced proliferation of dentate cells in gerbils. Neuroreport 12:915–917.

Lin H, Lin TN, Cheung WM, Nian GM, Tseng PH, Chen SF, Chen JJ, Shyue SK, Liou JY, Wu CW, Wu KK. 2002. Cyclooxygenase-1 and bicistronic cyclooxygenase-1/prostacyclin synthase gene transfer protect against ischemic cerebral infarction. Circulation 105:1962–1969.

Liu J, Solway K, Messing RO, Sharp FR. 1998. Increased neurogenesis in the dentate gyrus after transient global ischemia in gerbils. J Neurosci 18:7768–7778.

Markakis EA, Gage FH. 1999. Adult-generated neurons in the dentate gyrus send axonal projections to field CA3 and are surrounded by synaptic vesicles. J Comp Neurol 406:449–460.

Masferrer JL, Zweifel BS, Manning PT, Hauser SD, Leahy KM, Smith WG, Isakson PC, Seibert K. 1994. Selective inhibition of inducible cyclooxygenase 2 in vivo is antiinflammatory and nonulcerogenic. Proc Natl Acad Sci USA 91:3228–3232.

Matsuoka Y, Okazaki M, Zhao H, Asai S, Ishikawa K, Kitamura Y. 1999. Phosphorylation of c-Jun and its localization with heme oxygenase-1 and cyclooxygenase-2 in CA1 pyramidal neurons after transient forebrain ischemia. J Cereb Blood Flow Metab 19:1247–1255.

Miettinen S, Fusco FR, Yrjanheikki J, Keinanen R, Hirvonen T, Roivainen R, Narhi M, Hokfelt T, Koistinaho J. 1997. Spreading depression and focal brain ischemia induce cyclooxygenase-2 in cortical neurons through *N*-methyl-D-aspartic acid-receptors and phospholipase A2. Proc Natl Acad Sci USA 94:6500–6505.

Mirjany M, Ho L, Pasinetti GM. 2002. Role of cyclooxygenase-2 in neuronal cell cycle activity and glutamate-mediated excitotoxicity. J Pharmacol Exp Ther 301:494–500.

Morita I, Schindler M, Regier MK, Otto JC, Hori T, DeWitt DL, Smith WL. 1995. Different intracellular locations for prostaglandin endoperoxide H synthase-1 and -2. J Biol Chem 270:10902–10908.

Nakatomi H, Kuriu T, Okabe S, Yamamoto S, Hatano O, Kawahara N, Tamura A, Kirino T, Nakafuku M. 2002. Regeneration of hippocampal pyramidal neurons after ischemic brain injury by recruitment of endogenous neural progenitors. Cell 110:429–441.

Nogawa S, Zhang F, Ross ME, Iadecola C. 1997. Cyclo-oxygenase-2 gene expression in neurons contributes to ischemic brain damage. J Neurosci 17:2746–2755.

Ohtsuki T, Kitagawa K, Yamagata K, Mandai K, Mabuchi T, Matsushita K, Yanagihara T, Matsumoto M. 1996. Induction of cyclooxygenase-2 mRNA in gerbil hippocampal neurons after transient forebrain ischemia. Brain Res 736:353–356.

Okano HJ, Pfaff DW, Gibbs RB. 1996. Expression of EGFR-, p75NGFR-, and PSTAIR (cdc2)-like immunoreactivity by proliferating cells in the adult rat hippocampal formation and forebrain. Dev Neurosci 18:199–209.

Pai R, Soreghan B, Szabo IL, Pavelka M, Baatar D, Tarnawski AS. 2002. Prostaglandin E2 transactivates EGF receptor: a novel mechanism for promoting colon cancer growth and gastrointestinal hypertrophy. Nat Med 8:289–293.

Parent JM, Yu TW, Leibowitz RT, Geschwind DH, Sloviter RS, Lowenstein DH. 1997. Dentate granule cell neurogenesis is increased by seizures and contributes to aberrant network reorganization in the adult rat hippocampus. J Neurosci 17:3727–3738.

Reitz DB, Li JJ, Norton MB, Reinhard EJ, Collins JT, Anderson GD, Gregory SA, Koboldt CM, Perkins WE, Seibert K, et al.. 1994. Selective cyclooxygenase inhibitors: novel 1,2-diarylcyclopentenes are potent and orally active COX-2 inhibitors. J Med Chem 37:3878–3881.

Reynolds BA, Weiss S. 1992. Generation of neurons and astrocytes from isolated cells of the adult mammalian central nervous system. Science 255:1707–1710.

Sakakibara S, Imai T, Hamaguchi K, Okabe M, Aruga J, Nakajima K, Yasutomi D, Nagata T, Kurihara Y, Uesugi S, Miyata T, Ogawa M, Mikoshiba K, Okano H. 1996. Mouse-Musashi-1, a neural RNA-binding protein highly enriched in the mammalian CNS stem cell. Dev Biol 176:230–242.

Sakakibara S, Okano H. 1997. Expression of neural RNA-binding proteins in the postnatal CNS: implications of their roles in neuronal and glial cell development. J Neurosci 17:8300–8312.

Sandhya TL, Ong WY, Horrocks LA, Farooqui AA. 1998. A light and electron microscopic study of cytoplasmic phospholipase A2 and cyclooxygenase-2 in the hippocampus after kainate lesions. Brain Res 788:223–231.

Seaberg RM, van der Kooy D. 2002. Adult rodent neurogenic regions: the ventricular subependyma contains neural stem cells, but the dentate gyrus contains restricted progenitors. J Neurosci 22:1784–1793.

Seri B, Garcia-Verdugo JM, McEwen BS, Alvarez-Buylla A. 2001. Astrocytes give rise to new neurons in the adult mammalian hippocampus. J Neurosci 21:7153–7160.

Shono T, Tofilon PJ, Bruner JM, Owolabi O, Lang FF. 2001. Cyclooxygenase-2 expression in human gliomas: prognostic significance and molecular correlations. Cancer Res 61:4375–4381.

Skold M, Cullheim S, Hammarberg H, Piehl F, Suneson A, Lake S, Sjogren A, Walum E, Risling M. 2000. Induction of VEGF and VEGF receptors in the spinal cord after mechanical spinal injury and prostaglandin administration. Eur J Neurosci 12:3675–3686.

Smith WL, Garavito RM, DeWitt DL. 1996. Prostaglandin endoperoxide H synthases (cyclooxygenases)-1 and -2. J Biol Chem 271:33157–33160.

Song H, Stevens C, Gage F. 2002. Astroglia induce neurogenesis from adult neural stem cells. Nature 417:39–44.

Takagi Y, Nozaki K, Takahashi J, Yodoi J, Ishikawa M, Hashimoto N. 1999. Proliferation of neuronal precursor cells in the dentate gyrus is accelerated after transient forebrain ischemia in mice. Brain Res 831:283–287.

Takasawa K, Kitagawa K, Yagita Y, Sasaki T, Tanaka S, Matsushita K, Ohstuki T, Miyata T, Okano H, Hori M, Matsumoto M. 2002. Increased proliferation of neural progenitor cells but reduced survival of newborn cells in the contralateral hippocampus after focal cerebral ischemia in rats. J Cereb Blood Flow Metab 22:299–307.